



**THE STUDIES OF MITOCHONDRIA  
IN CULTURED CEREBELLAR GRANULE  
NEURONS: CHARACTERIZATION  
OF MITOCHONDRIAL FUNCTION,  
VOLUME HOMEOSTASIS AND  
INTERACTION WITH NEUROSTEROIDS**

**DZHAMILJA SAFIULINA**



TARTU UNIVERSITY  
PRESS

Department of Pharmacology, University of Tartu, Tartu, Estonia

Supervisors: Professor Alexander Zharkovsky, Department of Pharmacology,  
University of Tartu, Estonia

Dr. Allen Kaasik, Department of Pharmacology, University of  
Tartu, Estonia

Reviewers: Dr. Andres Piirsoo, Department of General and Molecular  
Pathology, University of Tartu, Estonia

Dr. Margus Pooga, Department of General Zoology, University  
of Tartu, Estonia

Dissertation is accepted for the commencement of the degree of Doctor of  
Philosophy in Neuroscience on January 27, 2006 by the Council for the  
Commencement of Doctoral Degree in Neuroscience

Opponent: Dr. Andrey V. Kuznetsov, Department of Transplant Surgery, D.  
Swarovski Research Laboratory, University Hospital Innsbruck,  
Austria

Commencement: February 27, 2006

Publication of this dissertation is granted by the University of Tartu

ISSN 1736–2792

ISBN 9949–11–256–7 (trükis)

ISBN 9949–11–257–5 (PDF)

Autoriõigus Dzhamilja Safiulina, 2006

Tartu Ülikooli Kirjastus

[www.tyk.ee](http://www.tyk.ee)

Tellimus nr 111

# TABLE OF CONTENTS

|  |    |
|--|----|
| LIST OF ORIGINAL PUBLICATIONS.....   | 7  |
| ABBREVIATIONS .....  | 8  |
| INTRODUCTION .....   | 10 |
| BACKGROUND OF THE STUDY .....  | 11 |
| Structure and function on the mitochondrion .....  | 11 |
| Mitochondrial dynamics.....  | 11 |
| Biogenesis of mitochondria.....  | 12 |
| Mitochondrial membrane potential and ATP synthesis by<br>mitochondria.....                                 | 12 |
| Ion transport across the mitochondrial membranes .....   | 13 |
| Mitochondrial $\text{Ca}^{2+}$ transport.....  | 13 |
| Regulation of mitochondrial function by calcium.....   | 14 |
| Mitochondrial $\text{K}^+$ cycle and volume regulation .....   | 14 |
| Cell death regulation .....  | 15 |
| The mitochondrial permeability transition pore: structure and<br>involvement in oxidative metabolism ..... | 15 |
| Steroid synthesis in mitochondria .....  | 16 |
| Cholesterol transport into the mitochondria and early steps of<br>steroidogenesis .....                    | 17 |
| Steroidogenesis in the brain .....   | 18 |
| Regulation of mitochondrial function by steroid hormones.....  | 19 |
| Mitochondria in neurons .....  | 20 |
| Motility of mitochondria in neurons .....  | 21 |
| Methods for studying mitochondrial function in neurons .....   | 22 |
| AIMS OF THE STUDY .....  | 23 |
| MATERIALS AND METHODS .....  | 24 |
| Reagents and solutions .....   | 24 |
| Cerebellar granule cell cultures .....   | 24 |
| Permeabilization of neurons.....   | 24 |
| Measurement of mitochondrial respiration.....  | 25 |
| Staining and fluorescence detection .....  | 25 |
| Visualization of mitochondria .....  | 25 |
| Visualization of cytoplasm and cytoskeleton .....  | 26 |
| Measurement of mitochondrial membrane potential.....   | 26 |
| Measurement of intramitochondrial $\text{Ca}^{2+}$ .....   | 27 |
| Time-course microscopy .....   | 27 |

|  |    |
|--|----|
| Deconvolution and image restoration.....   | 27 |
| 3D analysis of data .....  | 29 |
| Statistical analysis .....   | 29 |
| RESULTS .....  | 30 |
| Evaluation of mitochondrial function in situ in primary neuronal culture<br>of rat cerebellar granule cells..... | 30 |
| Characterization of permeabilized neuronal cultures .....  | 30 |
| Mitochondrial membrane potential .....   | 32 |
| Measurement of free calcium in mitochondrial matrix .....  | 33 |
| Mitochondrial respiration .....  | 34 |
| The effect of different steroids on neuronal mitochondria in model<br>of ischemia.....                           | 36 |
| Protective effect of different neurosteroids against calcium overload....  | 36 |
| DHEA effects on mitochondrial calcium accumulation .....   | 39 |
| Regulation of mitochondrial shape in cultured neurons .....  | 41 |
| Regulation of mitochondrial volume.....  | 41 |
| The effect of potassium ionophore valinomycin.....   | 42 |
| The effect of $K_{ATP}$ -channel opener pinacidil.....   | 42 |
| The effect of inhibitor of K/H exchanger.....  | 43 |
| The effect of uncoupling .....   | 43 |
| The effect of inhibition of respiratory chain .....  | 45 |
| Changes in mitochondrial volume affect the transport of mitochondria<br>in neurons .....                         | 46 |
| Reconstruction of mitochondria in neuronal processes and their<br>colocalization with cytoskeleton .....         | 48 |
| DISCUSSION.....  | 49 |
| Measurement of mitochondrial function in situ in permeabilized<br>neuronal cultures .....                        | 49 |
| Effect of neurosteroids on mitochondrial function.....   | 50 |
| Regulation of mitochondrial volume and it's physiological role<br>in neurons .....                               | 51 |
| CONCLUSIONS .....  | 54 |
| REFERENCES .....   | 55 |
| SUMMARY IN ESTONIAN .....  | 62 |
| ACKNOWLEDGEMENTS.....  | 64 |
| PUBLICATIONS .....   | 65 |

## LIST OF ORIGINAL PUBLICATIONS

- I Kaasik A, Safiulina D, Kalda A, Zharkovsky A. Dehydroepiandrosterone with other neurosteroids preserve neuronal mitochondria from calcium overload. *The Journal of Steroid Biochemistry and Molecular Biology*, 2003 Okt; 87(1): 97–103
- II Safiulina D, Kaasik A, Seppet E, Peet N, Zharkovsky A, Seppet E. Method for in situ detection of the mitochondrial function in neurons. *Journal of Neuroscience Methods*, 2004 Aug; 137(1):87–95
- III Safiulina D, Veksler V, Zharkovsky A, Kaasik A. Loss of mitochondrial membrane potential is associated with increase in mitochondrial volume: physiological role in neurons. *Journal of Cellular Physiology*. 2006 Feb; 206(2): 347–53

## ABBREVIATIONS

|                      |   |
|----------------------|---|
| 17- $\beta$ -HSD     | 17- $\beta$ -hydroxysteroid dehydrogenase                                 |
| 3- $\beta$ -HSD      | 3- $\beta$ -hydroxysteroid dehydrogenase                                  |
| Acetyl CoA           | acetyl coenzyme A   |
| ACTH                 | adrenocorticotrophic hormone  |
| ADP                  | adenosine diphosphate   |
| AIF                  | apoptosis-inducing factor   |
| ANOVA                | analysis of variance  |
| ANT                  | adenine nucleotide translocase  |
| Apaf-1               | apoptotic protease activating factor 1                                    |
| ATP                  | adenosine triphosphate  |
| Bak                  | Bcl-2 antagonist killer 1   |
| Bax                  | Bcl-2 associated X protein  |
| Bcl-2                | B-cell lymphoma 2   |
| BES                  | N,N-bis [2-hydroxyethyl]-2-aminoethanesulfonic acid                       |
| BSA                  | bovine serum albumin  |
| DHEA(S)              | dehydroepiandrosterone (sulphate)   |
| Drp1                 | dynamitin-related protein 1   |
| EGTA                 | ethylene glycol-bis( $\beta$ -aminoethyl ether)N,N,N',N'-tetraacetic acid |
| FADH <sub>2</sub>    | (1,5-dihydro-)-flavin adenine dinucleotide                                |
| FCCP                 | carbonylcyanide-p-trifluoromethoxyphenylhydrazone                         |
| GTP                  | guanosine triphosphate  |
| HEPES                | 4-(2-hydroxyethyl)-1-piperazine ethanesulfonic acid                       |
| KHC                  | kinesin 5B heavy chain  |
| KIF5B                | kinesin family member 5B  |
| MAP                  | microtubule-associated protein  |
| MES                  | 2-(N-morpholino)ethanesulfonic acid                                       |
| MitoK <sub>ATP</sub> | mitochondrial ATP-sensitive K <sup>+</sup> channel                        |
| MPP <sup>+</sup>     | 1-methyl-4-phenylpyridinium ion   |
| mPTP                 | mitochondrial permeability transition pore                                |
| mtDNA                | mitochondrial DNA   |
| NAD((P)H)            | (reduced) nicotinamide adenine dinucleotide (phosphate)                   |
| NRF                  | nuclear respiratory factor  |
| OPA1                 | optic atrophy 1   |
| P450 7B              | cytochrome P450 7 $\alpha$ ( $\beta$ )-hydroxylase                        |
| P450aro              | cytochrome P450 aromatase, CYP19A   |
| P450c11              | cytochrome P450 11-hydroxylase, CYP11B                                    |
| P450c17              | cytochrome P450 17- $\alpha$ -hydroxylase/c17,20-lyase, CYP17A1           |
| P450c21              | cytochrome P450 21-hydroxylase, CYP21                                     |

|                |   |
|----------------|---|
| P450sc         | cytochrome P450 cholesterol side-chain cleavage enzyme, CYP11A1       |
| PBR            | peripheral benzodiazepine receptor                                    |
| PGC-1          | peroxisome proliferator-activated receptor gamma, coactivator 1 alpha |
| PSF            | point spread function   |
| RCI            | respiratory control index   |
| StAR           | steroidogenic acute regulatory protein                                |
| TCA            | tricarboxylic acid cycle  |
| TMPD           | N,N,N',N'-tetramethylbenzene-1,4-diamine                              |
| VDAC           | voltage-dependent anion channel (mitochondrial porine)                |
| $\Delta\psi_m$ | mitochondrial membrane potential                                      |



## INTRODUCTION

Mitochondria are organelles, which are thought to be derived from symbiotic organisms that invaded eukaryotic cells early in evolution. They generate ATP, the major molecule by which cellular energy is transferred or spent. In neurons, mitochondria are presented in all compartments, including the axon. Translocation of mitochondria along axons is crucial to maintain proper functioning of the neuron, since oxidative phosphorylation is the main source of energy for neurons. Furthermore, during changes in respiratory activity mitochondria undergo transient changes in volume and morphology. Many neurodegenerative diseases, such as amyotrophic sclerosis, Alzheimer's, Huntington's, Parkinson's diseases, and Charcot-Marie-Tooth disease II, are related to defects in mitochondrial transport and/or disabled function.

Furthermore, mitochondria play a crucial role in the regulation of cell death. During ischemia calcium uptake by mitochondria is pivotal in controlling intracellular calcium concentration. Extensive calcium overload decreases mitochondrial membrane potential and ATP production, causes mitochondrial swelling and release of cytochrome C, leading to activation of apoptotic cell death pathways. Moreover, the inner mitochondrial membrane contains number of proteins, which are involved in regulation of programmed cell death.

Mitochondria are also known for housing the enzymes needed for hormone synthesis. The role of steroids in nervous system has been extensively studied since it was discovered, that steroid hormones can be synthesised in the nervous system independently of steroidogenic glands. These "neurosteroids" exert many effects on neuronal functions, including neuroprotection and neurotrophism. Several studies have shown that neurosteroids interact with mitochondria.

Therefore, in this thesis, the mitochondrial functioning in neurons and interaction of mitochondria with neurosteroids were studied.

# **BACKGROUND OF THE STUDY**

## **Structure and function on the mitochondrion**

Mitochondria are distinct organelles with two membranes, the inner and outer mitochondrial membranes which occasionally come together to form contact sites. The inner mitochondrial membrane is highly folded and largely impermeant forming the major barrier between the cytosol and the mitochondrial matrix. Multiple infoldings of the inner mitochondrial membrane form cristae which house a number of membrane bound mitochondrial enzymes. Mitochondrial matrix is enclosed by the inner membrane and contains mitochondrial DNA (mtDNA), ribosomes, matrix granules and matrix proteins. Also intermembrane space houses several proteins which are important in cell physiology, mitochondrial energetics and cell death. Additionally, the rate limiting enzymes of steroid synthesis are located in intermembrane space of mitochondria. The outer membrane is relatively permeant to small molecules and ionic species and contains a number of proteins, which are important for regulation of mitochondrial homeostasis.

## **Mitochondrial dynamics**

Mitochondria are remarkably dynamic organelles that undergo continual cycles of fusion and fission. These two processes continuously alter mitochondrial morphology in normal, non-apoptotic conditions (for instance, mitochondrial fission is required for cellular division). Disruption of fusion causes the tubular network of mitochondria to fragment into short rods or spheres (Gripatic et al., 2004; Chen and Chan, 2005), while disruption of fission (division) generates interconnected, perinuclearly clustered tubules (Smirnova et al., 2001; Stojanovski et al., 2004). The fission of mitochondria is regulated by large GTPases of the dynamin family, in particular, Drp1 (dynamin-related protein-1), and fusion by OPA1 (optic atrophy1) and mitofusins (Westermann, 2002; Yoon and McNiven, 2001). Two inherited neuropathies, Charcot–Marie–Tooth type 2A and autosomal dominant optic atrophy, are caused by mutations in mitofusin 2 and OPA1, suggesting that proper regulation of mitochondrial dynamics is particularly vital to neurons (Zuchner et al., 2004; Alexander et al., 2000).

## **Biogenesis of mitochondria**

Mitochondrial biogenesis is a critical process for development and cellular homeostasis. It involves expression of genes encoded in two different compartments, nucleus and mitochondria. Mitochondrial DNA encode only 13 polypeptides, while the exact number of mitochondrial proteins is not known, but estimates approximately 1000 proteins, 400 of which are currently identified (Mootha et al., 2003; Ozawa et al., 2003). Thus, nuclear genes play a predominant role in the biosynthesis of the respiratory chain and in the expression of the mitochondrial genome. Each mitochondrion has two to ten copies of the mtDNA molecule and the number of mtDNA molecules is a limiting factor in mitochondrial fission. Mitochondrial replication is controlled by number of nucleus-encoded factors (nuclear respiratory factors, NRFs, PGC-1 family coactivators) providing a mechanism for linking respiratory chain expression to environmental conditions (Gleyzer et al., 2005). Mutations of mtDNA are being increasingly recognised in disease and may play an important role in the ageing process (Taylor and Turnbull, 2005).

## **Mitochondrial membrane potential and ATP synthesis by mitochondria**

Mitochondrion contains two main enzymatic systems: the citric acid or tricarboxylic acid (TCA) cycle and the respiratory or electron transport chain (depicted in Figure 1).

The enzymes of TCA cycle break down acetyl CoA, derived from pyruvate and fatty acid breakdown to reduce  $\text{NAD}^+$  to  $\text{NADH}$  and  $\text{FAD}^{2+}$  to  $\text{FADH}_2$ . These intermediates provide reducing equivalents to the respiratory chain. In the respiratory chain electrons are transferred from  $\text{NADH}$  and  $\text{FADH}_2$  to Complexes I, and Complex II respectively, and these each then transfer electrons to ubiquinone which shuttles electrons to Complex III. Cytochrome c then shuttles electrons to Complex IV. These reactions are also associated with the transfer of protons across the mitochondrial inner membrane, from matrix into the inter-membrane space, establishing an electrochemical proton gradient, expressed as a mitochondrial transmembrane potential ( $\Delta\psi_m$ ).  $\Delta\psi_m$  is usually estimated at 150 to 180 mV negative to the cytosol. The mitochondrial membrane potential provides a force that drives the influx of protons into the mitochondria down the electrochemical potential gradient. The influx of protons is predominantly directed through the proton channel of the  $\text{F}_1\text{F}_0$ -ATP synthase, where inward movement of protons drives a motor of the enzyme to phosphorylate ADP and to release ATP (Stock et al., 1999). ATP is then transported out of the mitochondria by the adenine nucleotide translocase (ANT).

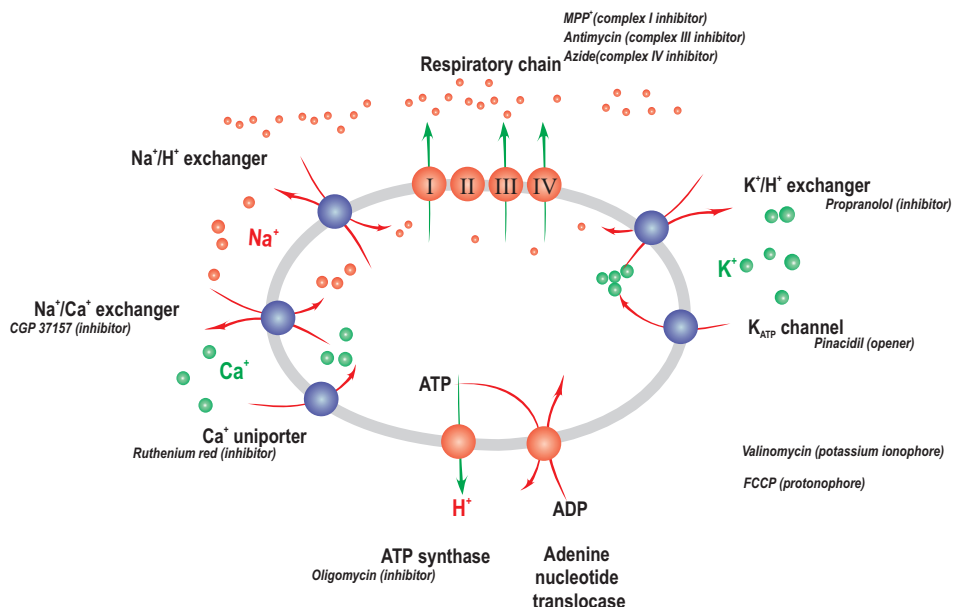


**Figure 1.** Schematic representation of mitochondrial respiratory chain and ion fluxes

## Ion transport across the mitochondrial membranes

### Mitochondrial $\text{Ca}^{2+}$ transport

The mitochondrial potential provides one of the major mechanisms to handle calcium in the cell.  $\text{Ca}^{2+}$  transport across the mitochondrial inner membrane is facilitated by specialized transporters as well as through the mitochondrial permeability transition pore (mPTP).  $\text{Ca}^{2+}$  is taken up through the mitochondrial inner membrane by a uniporter, which transports  $\text{Ca}^{2+}$  down its electrochemical gradient. The “rapid mode” of  $\text{Ca}^{2+}$  influx into the mitochondria was described, which could be an alternate configuration of the uniporter (Gunter et al., 2000). The mitochondrial outer membrane modulates the access of  $\text{Ca}^{2+}$  to the uniporter through the selectivity filter of the voltage-dependent anion channel (VDAC) which appears to be  $\text{Ca}^{2+}$  permeant. The major route for  $\text{Ca}^{2+}$  efflux from mitochondria is a  $\text{Na}^+/\text{Ca}^{2+}$  exchange. However,  $\text{Na}^+$  independent pathway dominates in liver mitochondria (Gunter et al., 1991).

## Regulation of mitochondrial function by calcium

The major functional significance of mitochondrial  $\text{Ca}^{2+}$  uptake is in the regulation of mitochondrial metabolism. Three major enzymes of the TCA are upregulated by  $\text{Ca}^{2+}$  (McCormack et al., 1990): pyruvate dehydrogenase, isocitrate dehydrogenase and  $\alpha$ -ketoglutarate dehydrogenase. More recently, direct increase of mitochondrial ATP production by mitochondrial  $\text{Ca}^{2+}$  uptake was shown (Jouaville et al., 1999). The electron transport chain, the  $\text{F}_0\text{F}_1\text{ATPase}$ , and the ANT have been suggested to be regulated by  $\text{Ca}^{2+}$  stimulation (Gunter et al., 2000). The glutamate/aspartate carrier, responsible for the transport of mitochondrial substrate, is also upregulated by calcium (Lasorsa et al., 2003). It therefore seems that the transfer of  $\text{Ca}^{2+}$  from the cytosol to mitochondria represents a major mechanism to couple increased ATP demand with an increase in the supply.

## Mitochondrial $\text{K}^+$ cycle and volume regulation

The outer membrane does not present a barrier to exchange of small ions with the cytosol and potassium flow is regulated in the level of inner mitochondrial membrane. Membrane potential drives  $\text{K}^+$  influx by diffusion (" $\text{K}^+$  leak") and via the mitochondrial  $\text{K}^+$  channels. Excess matrix  $\text{K}^+$  is ejected by the  $\text{K}^+/\text{H}^+$  antiporter.

It is well established that mitochondrial volume is mainly controlled by the mitochondrial potassium cycle as any *net*  $\text{K}^+$  flux will be accompanied by a flux of anions and osmotically obliged water. The balance of potassium influx and efflux processes depends on mitochondrial membrane potential. The negative internal mitochondrial membrane potential drives  $\text{K}^+$  as well as other cationic compounds electrophoretically into the mitochondrial matrix. Potassium extrusion via  $\text{K}^+/\text{H}^+$  antiporter, although electroneutral, requires the proton gradient that creates the membrane potential. As a result, a loss of membrane potential would thus lead to a decreased potassium influx into the mitochondrial matrix and also to an inhibition of its extrusion from the mitochondrial matrix. *A priori* it is not therefore possible to predict the net  $\text{K}^+$  displacement and concomitant volume change when the potential drops. It has been suggested that a high membrane potential corresponds to the swollen state and that when the potential collapses the mitochondria contract (Garlid and Paucek, 2003). In contrast, several works based on fluorescence microscopy studies suggest that mitochondria swell when they lose their membrane potential (Gao et al., 2001; Minamikawa et al., 1999; Lyamzaev et al., 2004), although others reported no volume change or small change (Kahlert and Reiser, 2002; Rintoul et al., 2003).

## Cell death regulation

Given the fundamental role of mitochondria as ATP generators it seems self-evident that severe damage to mitochondria will cause cell death. As ATP levels fall, energy dependent processes that include the maintenance of ion gradients, the contraction of muscle, secretion of transmitters, and the maintenance of normal regulation of calcium required for the coordination of calcium signals will inevitably become disordered. Once ionic gradients dissipate, intracellular osmolarity cannot be maintained, and cells will swell and die by a process of necrosis.

Furthermore, mitochondrion hosts key machinery for programmed cell death. The major form of apoptosis proceeds through the mitochondrial pathway, defined by a pivotal event in this process – mitochondrial outer membrane permeabilization. This leads to the release of proteins normally found in the space between the inner and outer mitochondrial membranes (including cytochrome c, apoptosis-inducing factor (AIF), and others). Before, during, or after permeabilization of outer membrane, there is frequently a dissipation of the mitochondrial membrane potential. Three general mechanisms precipitate the death of the cell: the release of molecules involved in the activation of caspases; the release of molecules involved in caspase-independent cell death; and the loss of mitochondrial functions essential for cell survival mentioned above.

### The mitochondrial permeability transition pore: structure and involvement in oxidative metabolism

The mitochondrial permeability transition pore (mPTP), also known as the megachannel or multiple conductance channel, is a multiprotein complex formed at the contact site between the inner and outer mitochondrial membranes, which helps regulate matrix  $\text{Ca}^{2+}$  concentrations, pH,  $\Delta\psi_m$  and mitochondrial volume. The open channel has a diameter of 1.0–1.3 nm and allows passage of solutes with molecular masses up to 1.5 kDa (Crompton, 1999). Opening of the mPTP is tightly regulated by  $\Delta\psi_m$  and matrix pH, and can be specifically inhibited by cyclosporin A, bongkreikic acid, EDTA or magnesium (Kroemer and Reed, 2000).

The exact composition of the mPTP is not clearly established. Six proteins have been implicated in either pore formation or its regulation: hexokinase, located in the cytosol; VDAC in the outer membrane; creatine kinase in the intermembrane space; the ANT in the inner membrane; cyclophilin D in the matrix, and the peripheral benzodiazepine receptor (PBR). The VDAC, an abundant protein in the mitochondria, comprising as much as 20% of outer membrane protein, is ordinarily open and allows diffusion of metabolites (<1kDa) across the mitochondrial outer membrane. The ANT is a specific antiporter for the exchange of ATP and ADP as part of oxidative phosphorylation.

Hexokinase converts glucose to glucose-6-phosphate, the initial phosphorylated intermediate of the glycolytic pathway. Creatine kinase facilitates the production and export into the cytosol of phosphocreatine, which enters the creatine/phosphocreatine circuit, thereby providing an efficient energy buffering and transport system connecting mitochondria with energy consumption sites (ATPases). Recent evidence has shown that the mPTP can form in the absence of the ANT (Kokoszka et al., 2004), and alternative models accounting for this pore have been proposed (He and Lemasters, 2002).

In ischemic injury permeabilization of mitochondrial membranes occur as a consequence of prolonged opening of the mPTP, resulting in a loss of inner membrane function and swelling of the matrix. The second class of mechanism for mitochondrial cell death is mediated by members of the Bcl-2 family of apoptosis-regulating proteins acting directly on the outer mitochondrial membrane. Anti-apoptotic Bcl-2 family members function to block mitochondrial permeabilization, whereas the various pro-apoptotic members like Bax and Bak promote it. Permeabilization releases proapoptotic factors, including cytochrome *c*, which participates in assembly of a caspase-activating complex between caspase 9 and Apaf-1 (“the apoptosome”) that activates effector caspases by cleavage, resulting in widespread proteolysis (Kroemer and Reed, 2000).

### **Steroid synthesis in mitochondria**

One particularly intriguing function of mitochondrial enzymes is the synthesis of steroid hormones. Mammalian mitochondrial steroid hydroxylating enzymes belong to cytochrome P450 enzyme superfamily. Enzymes of this superfamily are involved in the metabolism of chemically diverse endogenous and exogenous compounds, but also catalyze a wide variety of biosynthetic processes, including most steps in steroidogenesis. Type I P450 enzymes, found in mitochondria and bacteria, receive electrons from NADH via the intermediacy of two proteins-ferredoxin reductase (a flavoprotein) and ferredoxin (an iron/sulfur protein). Type I P450 enzymes involved in steroidogenesis include the cholesterol side-chain cleavage enzyme (P450<sub>scc</sub>), the two isozymes of 11-hydroxylase (necessary for cortisol synthesis), and several vitamin D-metabolizing enzymes. Type II P450 enzymes, found in the endoplasmic reticulum of eucaryotes, receive electrons from NADPH via P450 oxidoreductase, which contains two flavin moieties. Steroidogenic Type II P450 enzymes include 17- $\alpha$ -hydroxylase/c17,20-lyase (P450<sub>c17</sub>), 21-hydroxylase (P450<sub>c21</sub>), and aromatase (P450<sub>aro</sub>) (Miller, 2005).

## Cholesterol transport into the mitochondria and early steps of steroidogenesis

The initial steps of the synthesis of all steroids are common to all steroidogenic tissues, such as adrenal, gonad and placenta tissues, and also to the brain tissue. First, cholesterol is transported to the inner membrane of mitochondria via peripheral benzodiazepine receptor (PBR). The PBR was first identified as a binding site for the benzodiazepine, diazepam, in peripheral organ systems, and subsequently was found to be distinct from the benzodiazepine binding site in the central nervous system. The PBR is widely expressed throughout the body, with highest densities found in steroid-producing tissues. The 18kDa PBR protein contains 169 amino acids and form five transmembrane  $\alpha$ -helices spanning the outer mitochondrial membrane, which function as a channel for cholesterol (Papadopoulos et al., 1997). A region of the cytosolic carboxyl-terminus of the receptor was identified as the cholesterol binding site (Li and Papadopoulos, 1998).

Further, the steroidogenic acute regulatory protein (StAR) is necessary for mobilization of cholesterol from the outer to the inner contact sites of mitochondrial membranes. In gonadal and adrenal cells, StAR protein is newly synthesized in response to trophic hormones (ACTH, gonadotropins) and this synthesis parallels the maximal steroid synthesis in response to hormones. The cytosolic precursor of StAR protein is cleaved at the level of the mitochondrial membrane contact sites to produce the 30 kDa mitochondrial "mature" StAR protein, which is responsible for cholesterol transport across the mitochondrial membranes (King et al., 1995). Recent studies have shown that StAR is present in different regions of mammalian brain (Furukawa et al., 1998, Kim et al., 2004). Additional factors have been identified in different tissues (Liu et al., 2003) and in the brain (Sierra, 2004), indicating that the StAR it might not be limiting and that other mitochondrial membrane components participate in inducing and maintaining continuous steroid formation.

The first step in biosynthetic pathway is cholesterol conversion to pregnenolone by the C27 cholesterol side chain cleavage cytochrome P450 enzyme (P450<sub>scc</sub> or CYP11A1). Pregnenolone then leaves the mitochondrion to undergo enzymatic transformation in the endoplasmic reticulum that will give rise to the final steroid products. Next biosynthetic steps are different depending on particular tissue.

Studies show, that not the P450<sub>scc</sub> enzyme activity, but cholesterol transport to the inner mitochondrial membrane is the rate-limiting step in synthesis of steroid hormones (Papadopoulos et al., 1997).



## Steroidogenesis in the brain

In the brain, glial cells are considered to be the primary site for steroid synthesis. However, the presence and activity of steroidogenic enzymes are demonstrated also in neuronal cells (Shibuya et al., 2003, Tsutsui et al., 2004). Sex steroids, both androgens and estrogens, are made via synthesis of dehydroepiandrosterone (DHEA) or progesterone. The cleavage of pregnenolone to DHEA in adrenals and gonads requires both the 17 $\alpha$ -hydroxylase and 17, 20-lyase activities of P450c17, which is found in the endoplasmic reticulum. Only a transient expression of mRNA for P450c17 during embryonic life was reported (Compagnone et al., 1995) and contradictory data on the presence of its mRNA and activity in adult brain has been presented (Stromstedt et al., 1995; Sanne and Krueger, 1995; Kohchi et al., 1998). A possible alternative pathway for DHEA synthesis involving oxygenated hydroxyperoxides has been suggested since oxidative stress lead to increased DHEA production (Cascio et al., 1998, Maayan et al., 2005). Nevertheless, DHEA and other steroid hormone precursors/metabolites are found in the brain in relatively high concentrations. Furthermore, their levels in the brain do not change after several weeks after removal of steroidogenic glands (Corpechot et al., 1981). Such steroids synthesized in the brain are called neurosteroids (Baulieu, 1998).

The progesterone synthesizing enzyme, microsomal 3 $\beta$ -hydroxysteroid dehydrogenase, catalyses also oxidation of DHEA to yield androstendione, which is further converted to testosterone and estradiol by 17- $\beta$ -hydroxysteroid dehydrogenase and P450aromatase. In the brain, the prominent pathway of DHEA metabolism is hydroxylation in 7th position by P450 7B yielding 7- $\alpha$ ( $\beta$ )-hydroxy-DHEA, which is converted to 7-oxo-DHEA by 11- $\beta$ -hydroxysteroid dehydrogenase type 1. These 7-oxo-steroids are not further convertible to either estrogen or testosterone. Possible pathways of steroid synthesis in the brain are shown in Figure 2.

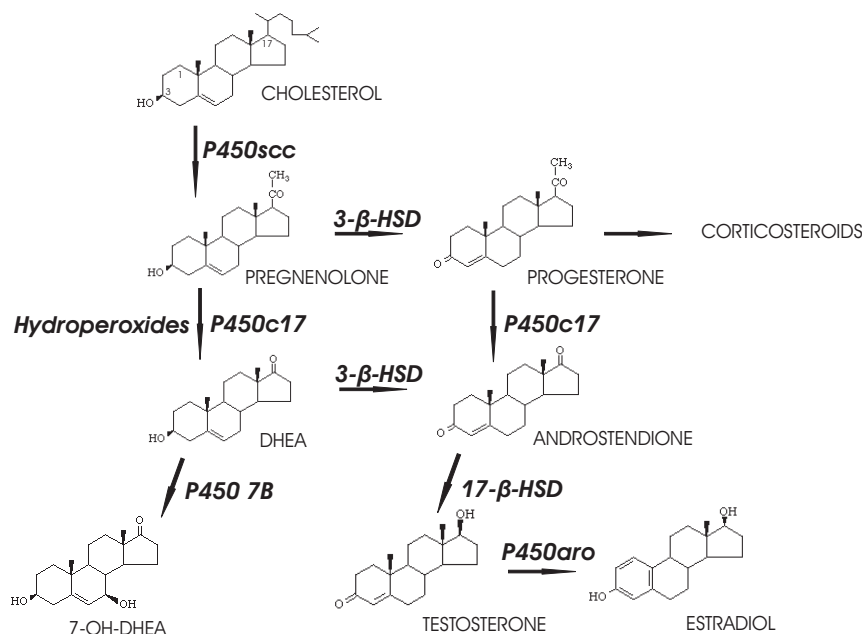


**Figure 2.** Biosynthesis and metabolism of steroids in the brain. Sulfatation reactions of pregnenolone and dehydroepiandrosterone (DHEA) mediated by sulfontransferase/sulfatase and further conversion of 7- $\alpha$ ( $\beta$ )-hydroxy-DHEA to 7-oxo-DHEA by 11- $\beta$ -hydroxysteroid dehydrogenase are not shown. Cytochrome P450 enzymes: P450scc cholesterol side-chain cleavage enzyme; 3- $\beta$ -HSD-3- $\beta$ -hydroxysteroid dehydrogenase; P450c17-17- $\alpha$ -hydroxylase/c17,20-lyase; P450 7B-7- $\alpha$ ( $\beta$ )-hydroxylase; 17- $\beta$ -HSD-17- $\beta$ -hydroxysteroid dehydrogenase; P450aro-aromatase.

### Regulation of mitochondrial function by steroid hormones

Despite of tight relationship between mitochondria and steroid synthesis the functional significance of this interaction remains unclear. Estradiol binds specifically to isolated brain synaptosomal mitochondria with  $K_m$  in around of 10nM (Horvat et al., 2001). Also glucocorticoid receptor was found in rat brain mitochondria (Moutsatsou et al., 2001). The action of estrogens and glucocorticoids could be related with regulation of mitochondrial gene expression. Recent studies indicate, that steroid hormones regulate expression of the genes involved in oxidative phosphorylation coded in mitochondrial as well as in nuclear genome (Damschroder-Williams et al., 2005; Masri 2005). Moreover, steroids affect mitochondrial function directly. Morin et al. (2000) recently demonstrated that DHEA and  $\alpha$ -estradiol partly preserve the function of isolated mitochondria altered by anoxia-reoxygenation. DHEAS also preserves the loss of mitochondrial activity following exposure of neurons to ischemic insult (Kaasik et al., 2001). Several other steroids have been shown to preserve mito-

chondrial transmembrane potential after exposure of cells to toxic insults (Mattson et al., 1997, Wang et al., 2001). Estradiol inhibits Na-dependent  $\text{Ca}^{2+}$  efflux from mitochondria (Horvat et al., 2001). Another action of estradiol on mitochondria is inhibition of  $\text{F}_0\text{F}_1$  ATPase by binding to oligomycin sensitivity conferring protein, subunit of this enzyme (Zheng and Ramirez, 1999). DHEA and  $\alpha$ -estradiol were able to intercalate into the phospholipid bilayers, leading to structural and functional membrane modifications (Golden et al., 1998). In micromolar concentrations DHEA and related steroids inhibit oxygen consumption with NADH related substrates in mitochondria isolated from different tissues (Mohan and Cleary, 1989).

## Mitochondria in neurons

Mitochondria vary across different tissues: classical electron microscopy studies have demonstrated morphological differences in mitochondria from different cell types. In neurons mitochondria appear oval in shape on electron microscopy images (Frey et al., 2002) and thread-like when visualized by confocal microscope (Rintoul et al., 2003). Also mitochondrial enzymatic and biosynthetic pathways are different in different tissues (Thorburn, 2004). As an example, neuronal mitochondria lack any capacity for  $\beta$ -oxidation, the process by which fatty acids are broken down in the mitochondria to generate acetyl CoA, the entry molecule for the TCA (Yang et al., 1987). Brain mitochondria are also functionally heterogeneous varying in different cell types (neuronal, glial) and brain regions (Davey et al., 1997). In mitochondria of synaptic origin, complex I activity has a major control of oxidative phosphorylation, such that when a threshold of 25% inhibition is exceeded, energy metabolism is severely impaired, resulting in a reduced synthesis of ATP (Davey et al., 1998). On the other hand, whole brain mitochondria oxidative phosphorylation is under control of phosphorylation level by ATP synthase (Rossignol et al., 2000). These variations can be explained by tissue- and cell-specific expression of subunits of oxidative phosphorylation system (Kunz, 2003).

Growing evidence suggests a crucial role of mitochondrial dysfunction in the pathogenesis of neurologic diseases (reviewed by Beal, 2000; Schon and Manfredi, 2003). For example, the defects in respiratory chain resulting in insufficient energy production and excess oxygen radical generation form a basis for neurodegenerative disorders such as the Parkinson's, Alzheimer's and Huntington's diseases (Schon and Manfredi, 2003) and the stroke-like episodes (Sims and Anderson, 2002). Even if mitochondrial dysfunction manifests as an epiphenomenon, it can precipitate the cascade of events leading to the cell's death (Tatton and Olanow, 1999). Therefore, understanding the role and mechanisms of involvement of mitochondria in neurologic diseases is of principal importance for elaborating the optimal therapeutic strategies.

## **Motility of mitochondria in neurons**

The proper intracellular distribution of mitochondria is crucial for the normal physiology of neurons. Mitochondria undergo saltatory and bidirectional movements with velocities of 0.3–2.0  $\mu\text{m sec}^{-1}$  (Overly, 1996; Ligon and Steward, 2000). Mitochondria accumulate near active growth cones of developing neurons (Morris and Hollenbeck, 1993), and invariably are present within the synaptic terminals (Shepherd and Harris, 1998). Dendritically distributed mitochondria play an essential role for the support of synapse density and plasticity (Li et al., 2004). Mitochondria in the cell bodies of neurons are transported down the neuronal processes in response to changes in the local energy state and metabolic demand (Hollenbeck, 1996). Because of their extreme polarity, neurons require specialized mechanisms to regulate the transport, targeting, and retention of mitochondria at specific subcellular locations. Thus, efficient control of mitochondrial distribution and transport in response to cellular processes and stimuli is essential for neuronal development and synaptic function.

The kinesin family of molecular motors is responsible for anterograde transport of axonal mitochondria, whereas members of the cytoplasmic dynein family are the driving force behind retrograde movement (Hollenbeck, 1996; Ligon and Steward, 2000). Although the need for multiple kinesins in axonal transport of mitochondria is unclear, KIF5B (kinesin 5B; KHC) is believed to be a key molecular motor for driving anterograde mitochondrial movement in neurons. However, how these motors interact dynamically with mitochondrial membranes, and how trafficking components, including molecular motors, linkers (or adaptors), and receptors of mitochondria, are assembled into transport machinery are poorly understood. Recently, one component of mitochondrial transport machinery has been described. Syntabulin, a syntaxin-binding protein that links syntaxin-containing vesicles to KHC, associates with mitochondria *in vivo* and links these organelles to KIF5B (Cai et al., 2005). This association mediates mitochondrial trafficking along axonal processes, and consequently, contributes to proper distribution of mitochondria in neurons. Linkage to the right adaptors and motors is a key decision, but even if that is achieved, movement in the right direction is not ensured unless an open path is provided. The control over traffic by phosphorylation has been suspected to contribute to the regulation. Axonal microtubules provide the track for organelle transport and microtubule associated proteins (MAPs) regulate organelle transport. Activation of protein kinase pathways and phosphorylation of MAPs reduces their interaction with microtubules thus facilitating organelle transport (Sato-Harada et al., 1996; Mandelkow et al., 2004). Also phosphorylation state of kinesin and associated proteins may regulate motility via association with organelle membranes (Lee and Hollenbeck, 1995).

## Methods for studying mitochondrial function in neurons

Conventional studies of neuronal mitochondria have been limited to usage of purified preparations of isolated mitochondria (Lee, 1995), neural cell homogenates (Atlante et al., 1998, 1999), living neurons (Dedov et al., 2001), and brain slices (Gähwiler et al., 1997; Kudin et al., 1999).

The analysis of the biochemical and bioenergetic principles are generally based on studies of mitochondria isolated in bulk from tissues such as the liver, the heart or the brain. Mitochondria are purified, and biochemical functions such as the rate of oxygen consumption, the rate of production of biochemical intermediates etc. are assessed. While such work provides the mainstay for our understanding of mitochondrial bioenergetics, it also has its limitations. Most obviously, under these conditions, it is impossible to ask questions about the specialization of mitochondrial function in different cell types. It is certainly not possible to study spatial and temporal changes in mitochondrial function in a single cell during events associated with cell signalling or in response to pathophysiological conditions. Moreover, the preparation of mitochondrial fraction requires significant amounts of tissue for being homogenized that makes it impossible to analyze the mitochondria in distinct regions or cell types. Estimation of mitochondrial function in living cells and tissue slices, either by measuring oxygen utilization or visualization of mitochondrial membrane potential and calcium levels, also bears the problems. Although it describes the cellular metabolic status, no meaningful information regarding the regulation of the processes of energy production and utilization can be derived. For example, it is impossible to analyze the kinetics of regulation of mitochondrial respiration by ADP, since intracellular concentrations of this compound cannot be directly monitored *in vivo*, and while added exogenously, it does not reach the mitochondria through the impermeable cellular membrane. Likewise, it is difficult to discriminate primarily occurring mitochondrial disorders from those secondarily caused by cellular dysfunction (Saks et al., 1998). These drawbacks have promoted a search for the methods of *in situ* studies. In this respect, the permeabilized cell technique, effectively applied in muscle research (Veksler et al., 1987; Saks et al. 1998) offers a number of advantages. First, it allows to investigate all the mitochondria of the same and little amount of the specimen. It also provides information regarding the intactness of the mitochondrial inner and outer membranes and function of energy transfer systems connecting mitochondria with ATPases, both in normal and pathological conditions (Saks et al., 1998). At the same time the utility of using permeabilized neural cells in studies of the mitochondrial function *in situ* has not been demonstrated as yet. Therefore, in this thesis, the permeabilized primary cultures of cerebellar granule cells were used to characterize mitochondrial function concerning respiratory activity, calcium accumulation, interaction with neurosteroids, and mitochondrial volume regulation and motility in neuronal processes.

## **AIMS OF THE STUDY**

1. To apply the permeabilization technique to cultured primary neurons to study the mitochondrial function *in situ*.
2. To estimate whether the neurosteroids, especially dehydroepiandrosterone, affect the mitochondrial function in situ in permeabilized neurons.
3. To elucidate the mechanisms and potential physiological role of mitochondrial volume changes in neurons.

## MATERIALS AND METHODS

### Reagents and solutions

All reagents were purchased from Sigma-Aldrich (MO, USA) except the fluorescence dyes and Pluronic which were obtained from Molecular Probes (OR, USA). *Solution 1* contained (in mM): 7.23 potassium ethylene glycol-bis( $\beta$ -aminoethyl ether)N,N,N',N'-tetraacetate ( $K_2$ EGTA), 2.77  $CaK_2$ EGTA, 60 N,N-bis [2-hydroxyethyl]-2-aminoethanesulfonic acid (BES), 5.69 MgATP (1 free  $Mg^{2+}$ ), 20 taurine, 3  $K_2HPO_4$ , 0.5 dithiothreitol and 81 potassium methanesulfonate, pH 7.1 at 25 °C. *Solution 2* contained (in mM): 7.23  $K_2$ EGTA, 2.77  $CaK_2$ EGTA, 100 potassium salt of 2-(N-morpholino)-ethanesulfonic acid (K-MES), 1.38  $MgCl_2$ , 20 taurine, 3  $K_2HPO_4$ , 0.5 dithiothreitol, 20 imidazole and 5 mg/ml bovine serum albumine (BSA), pH 7.1 at 25 °C. The stock solutions of ADP used to add ADP into solutions contained  $MgCl_2$  (0.6 mol/mol ADP) to avoid changes in the free  $Mg^{2+}$  concentrations. The concentrations of free  $Ca^{2+}$  were calculated using the computer program of Fabiato (Fabiato, 1988). Lockey solution contained (in mM): 90 Choline chloride, 30  $NaHCO_3$ , 0.1  $CaCl_2$ , 5 KCl, 3  $MgCl_2$ , 20 HEPES, 13.6 Glucose, pH 7.4.

### Cerebellar granule cell cultures

Primary cultures of rat cerebellar granule cells were prepared according to the method of Gallo *et al.* (1982), with minor modifications as described in papers I, II and III. The cell suspension was plated at a density  $1.0 \times 10^6$  cells/ml on poly-L-lysine coated LabTek II Chambered Coverglass (0.3 ml/chamber; Nalge Nunc International, NY, USA) or at a density  $1.25 \times 10^6$  cells/ml on poly-L-lysine coated MatTek Glass Bottom Culture Dishes (2ml; MatTek Corporation, MA, USA). The cells were cultured for 5–7 days in a humidified 5%  $CO_2$ /95% air at 37°C.

### Permeabilization of neurons

Permeabilization of the plasmalemma was obtained by incubating the cultures for 15 min at 4°C in *solution 1* at pCa 7 containing additionally 50  $\mu$ g/ml saponin. Cells were then rinsed once with the *solution 1*, in order to washout saponin, and kept for subsequent experiments. Alternatively, the cells were treated for 3 min at room temperature with 50  $\mu$ g/ml saponin in the same solution followed by washout.

## Measurement of mitochondrial respiration

The permeabilized neurons kept in *solution 1* were carefully scraped from the plate, centrifuged at 4 °C for 10 min at 3000 rpm, and resuspended in *solution 2*. Then the cells were transferred into the oxygraph medium (*solution 2*) complemented with 5 mM glutamate and 2 mM malate, with a final concentration of 5.66 million cells/ml and a total volume of 1.5 ml at 25°C. After registration of the basal respiration rate ( $V_0$ ), 2 mM ADP was added to maximally stimulate the respiration ( $V_{ADP}$ ) followed by addition of 5 mM  $\text{NaN}_3$  to inhibit the cytochrome oxidase complex. The similar experiments were performed also in the presence of either 10 mM succinate (in the presence of 10  $\mu\text{M}$  rotenone) to activate complex II or 0.5 mM  $\text{N,N,N',N'}$ -tetramethylbenzene-1,4-diamine (TMPD) and 2 mM ascorbate together with 8  $\mu\text{M}$  cytochrome c to maximally activate the cytochrome oxidase complex. In preliminary experiments started in the absence of exogenous cytochrome c, it induced approximately 10% increase in respiration when added into the oxygraph medium at the end of experiment. In following experiments cytochrome c was therefore added together with TMPD and ascorbate to ensure that cytochrome oxidase is by no means limited by availability of cytochrome c. Exogenous cytochrome c was not used with other substrates as in these cases respiration was not increased by the addition of cytochrome c, indicating that the outer mitochondrial membrane in permeabilized cells remained intact or that the loss of cytochrome c was not limiting step in these cases.

In all experiments the  $\text{NaN}_3$ -sensitive part of the ADP-stimulated respiration was taken to represent the activity of cytochrome oxidase. The respiratory control index (RCI) as a ratio between the rates of respiration after and prior to addition of saturating concentrations of ADP ( $V_{ADP}/V_0$ ) was calculated. The rates of oxygen uptake were recorded by using the high resolution respirometer (Oroboros Oxygraph, Paar KG, Graz, Austria) equipped with Clark oxygen sensor and with DATGRAPH analysis software.

## Staining and fluorescence detection

All microscopy procedures were performed using confocal laser scanning microscope (MRC1024, BioRad) equipped with Ar-Kr laser.

## Visualization of mitochondria

To visualize the integrity of mitochondrial membranes, the neurons were first loaded 30 min at 37°C with 100 nM MitoTracker Green in culture media that was followed by incubation in the presence of different saponin concentrations



for 15 min and washout as described above. Excitation line was 488nm and emission was monitored at 522 (DF35) nm.

For mitochondrial tracking the intact neurons were loaded for 120 min at 37°C with 100 nM MitoTracker Green in culture media.

### **Visualization of cytoplasm and cytoskeleton**

To assess the changes in plasma membrane integrity the cultures were first loaded with 1 µg/ml fluorescein diacetate added to the culture media for 7 min at 37°C, then processed for permeabilization and visualized by illuminating with the 488 nm and detecting emission at 522 (DF35) nm.

To stain the cytoplasm, intact neurons were loaded for 30 min with 5 µM CellTracker Green CMFDA (5-chloromethylfluorescein diacetate) at 37°C in Lockey's solution that was replaced with conditioned medium after staining.

For staining of microtubules, neurons were incubated with 2 µM Oregon Green 488 paclitaxel in conditioned medium for 30min and washed once after staining. Mitochondria were co-visualized with 200 nM MitoTracker Red. Excitation lines were 488nm and 568nm and emission at 522 (DF35) and 605 (DF32) nm, respectively, was monitored.

### **Measurement of mitochondrial membrane potential**

$\Delta\psi_m$  was estimated in permeabilized neurons loaded with the  $\Delta\psi_m$  sensitive fluorescent dye JC-1 (Molecular Probes, USA). The permeabilized cultures were first incubated for 10 min at room temperature on slowly 3D rotating rocker with *solution 1* containing mitochondrial substrates, 5 mM glutamate, 2 mM malate after what compounds of interest were added and incubation was continued for 10–20 min. Desired pCa was obtained by varying CaK<sub>2</sub>EGTA/K<sub>2</sub>EGTA. After that 3 µM JC-1 was added and incubation was proceeded for next 10 min. Fields of neurons (~300 cells) were illuminated with the 488 and 568 lines and emission at 522(DF35) and 605(DF32) nm was monitored. The fluorescent emission wavelength of JC-1 depends on the aggregation of the JC-1 molecules in mitochondria that in turn depends on the  $\Delta\psi_m$ . Relative changes in  $\Delta\psi_m$  were assessed by monitoring the ratio of JC-1 fluorescence at 605 nm (aggregate) and 522 nm (monomer) using the LaserSharp 2000 software (Biorad).

## Measurement of intramitochondrial $\text{Ca}^{2+}$

For quantitative measurement of mitochondrial  $\text{Ca}^{2+}$  signals, permeabilized neurons were loaded at room temperature for 20 min with 3  $\mu\text{M}$  X-rhod-5F-AM (*Molecular Probes, USA*) in *solution 1* and incubated at room temperature for 30 min to allow hydrolysis of X-rhod-5F-AM trapped in mitochondria. This was followed by 20 min incubation in *solution 1* containing compounds of interest at different pCa after what the dishes were mounted on the stage of laser scanning confocal microscope and illuminated with the 568-line and emission at 605(DF32) nm was monitored.

## Time-course microscopy

Mitochondrial motility was measured in intact cultures of cerebellar granule neurons loaded with MitoTracker Green by time-course confocal microscopy. Temperature in culture media was kept at 37°C with a temperature-controlled POC-Chamber system (LaCon, Staig, Germany) and 40x spring WLSM type objective (0.9 numerical aperture, Olympus) equipped with an objective heater. pH was maintained at 7.1 with 20 mM HEPES. Time-course analysis was performed using the LaserSharp 2000 software time-course option by recording 30 frames over 5 minutes. Coordinates of randomly chosen mitochondria were tracked through the time series and recorded by software registering the mouse clicks. Obtained data matrices were further processed in Microsoft Excel Macro calculating the percentage of time in motile state, percentage of time in stationary state, distance, average velocity in motile state, maximal velocity and average velocity for each mitochondria.

## Deconvolution and image restoration

512x512 pixel digital optical sections were taken with a confocal laser scanning microscope (MRC1024, BioRad) equipped with Ar-Kr laser emitting the excitation wavelengths of 488 and 568 nm utilizing a 100x oil immersion objective (1.35 numerical aperture, Olympus). Voxels were collected at 15 nm lateral and 100 nm axial intervals. According to the Nyquist theorem, these settings should result in a overlap between successive optical sections and ensure that no signal will be lost along the Z axis. Laser power was usually kept below 30  $\mu\text{W}$  (in exceptional cases 90  $\mu\text{W}$ ) and exposition time of single mitochondria to laser beam did not exceed 180 s.

Raw images were transferred to a MicroLink workstation equipped with Intel 3,00 GHz Hyper-Threading 800MHz Bus Prescott processor and 2GB random access memory and deconvolved by the AutoDeblur 9.2 software

package (AutoQuant Imaging, NY, USA). The software is based on blind deconvolution algorithm together with maximum likelihood estimation and produces point spread function (PSF) from information within dataset. Because the algorithm adjusts the point spread function to the data, it partially corrects also for spherical aberration. However, to eliminate this distortion completely, z-distances were corrected using scalar compensation factor [ (apparent diameter-aberration coefficient)/ apparent diameter]. Aberration coefficient was calculated from the images of green fluorescent microspheres (see below) and was 303 nm.

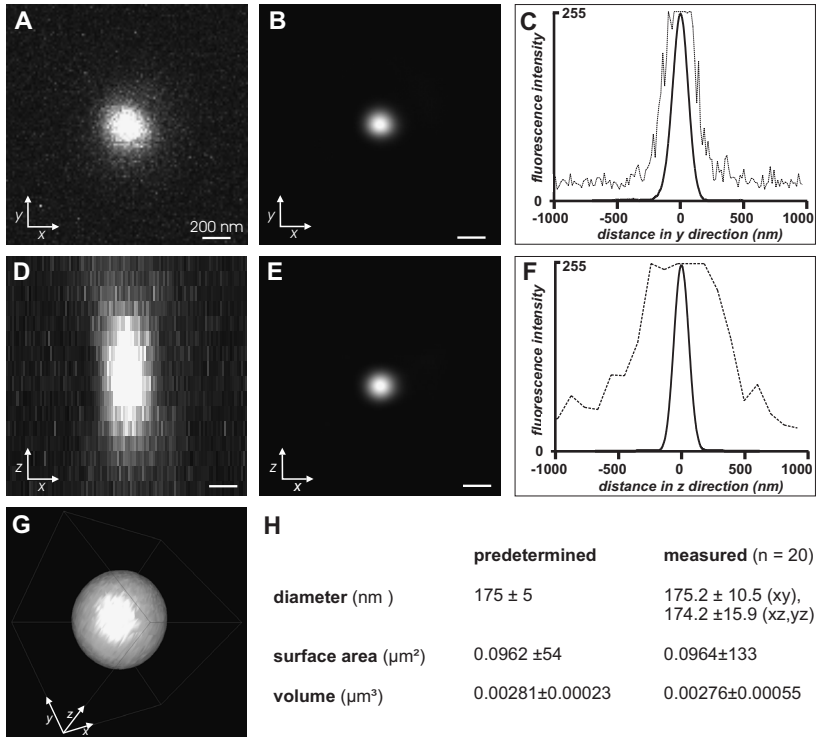


**Figure 3.** Imaging of subresolution fluorescent microspheres (ø175 nm). Panels A and D show maximal XY and XZ projections of raw image series, respectively. Note the spherical aberration present along the z axis in D. Panels B and E show the maximal XY and XZ projections of 3D deconvolved image series after correction of spherical aberration. Panels C and F depict the axial intensity profiles generated from these images before (dotted line) and after (solid line) image restoration. Panel G shows 3D isosurface reconstruction of the deconvolved image series (frame size 250 x 250 x 250 nm). Panel H compares the parameters of microspheres provided by the manufacturer with parameters measured from reconstructed images. Note that experimentally determined values correspond well with the manufacturer's values.

To assure the accuracy of these approaches, software settings were optimized with green fluorescent microspheres (Molecular Probes' PS-Speck Microscope Point Source Kit) having the constant diameter. Beads were first bleached with a high laser power to receive similar signal to noise ratio as in mitochondrial preparations and series of images were then recorded with identical parameter setting as used for mitochondrial images. Figure 3 summarizes the data restoration process. Panels A and D depict the projections of raw images in XY and XZ planes and panels B and E demonstrate the same images after data restoration process. Panels C and F show the axial intensity profiles generated from these images and panel G presents the final 3D isosurface picture generated from all slices. Table depicted in panel H shows that predetermined parameters of microspheres given by producer correspond very well with these measured by us from reconstructed images.

### **3D analysis of data**

Isosurface 3D pictures were generated using the AutoVisualize software package (AutoQuant Imaging) after binarizing with a fixed 32% threshold value. Mitochondrial length and diameter in optical plane was measured blindly from maximal XY projections of similarly binarized images. Maximal projections are superimpositions of all optical sections of deconvolved image stacks. Mitochondrial thickness along the optical axis was similarly determined from XZ or YZ projections. Surface area and volume was calculated automatically by AutoVisualize.

### **Statistical analysis**

The data are presented as mean  $\pm$  SEM. The Student t-test or one-way ANOVA and Bonferroni *post hoc* analysis was used to compare data in different groups.

## **RESULTS**

### **Evaluation of mitochondrial function in situ in primary neuronal culture of rat cerebellar granule cells**

#### **Characterization of permeabilized neuronal cultures**

The use of plant-origin detergents for permeabilization of the plasma membrane to characterize the functioning of intracellular membrane organelles is largely employed in the field of muscle bioenergetics (Saks et al, 1998). Originally, Endo and Kitazawa (1978) used 50 µg/ml concentration of saponin to permeabilize bundles of cardiac and skeletal muscle. Glycosides saponin and digitonin have high affinity for cholesterol and therefore specifically dissolve cholesterol-rich membranes such as plasma membrane. The selection of appropriate saponin concentration for selectively dissolve plasmalemma is crucial since saponin also disrupts the membranes of mitochondria at higher concentration.

The optimum saponin concentration for permeabilization was revealed by exposing the plated neuronal cultures to different saponin concentrations for 15 min and detecting the integrity of plasma membrane by monitoring fluorescein diacetate signal (Figure 4). It can be seen that the cultures without saponin and those with 10 µg/ml saponin emitted similar signal with fluorescein being typical for the cells with intact membranes. The first signs of permeabilization of the cells (leakage of cytoplasmic fluorescein) were observed after treatment of the cells with 25 µg/ml saponin, when the fluorescence signal became focally dissipated. Increasing of saponin concentrations to 50 µg/ml and higher values almost completely abolished the signal. At 100 µg/ml concentration of saponin the leakage was accompanied by detachment of the neurons and neurites from the plate.

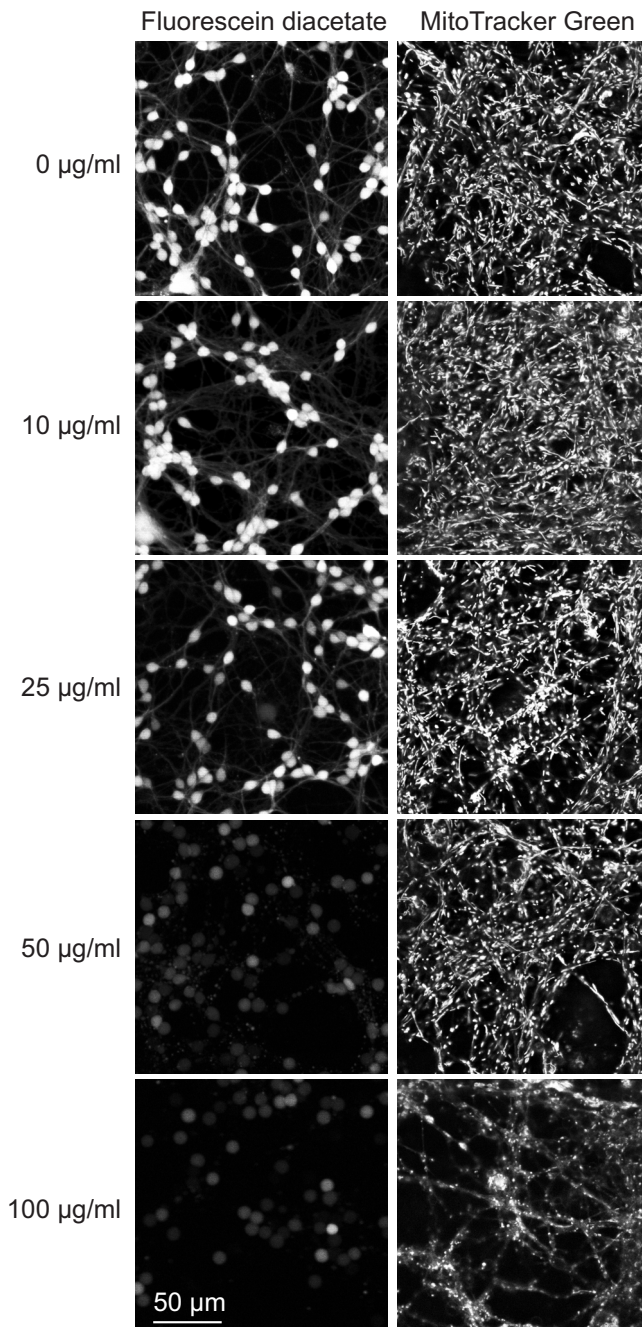


**Figure 4.** Cell membrane integrity (left column) of cerebellar granule neurons as stained by fluorescein diacetate and mitochondrial intactness (right column) as stained by MitoTracker Green) after 15 min incubation at different saponin concentrations (shown in left).

The integrity of the mitochondrial membranes was monitored using the potential-independent accumulation of MitoTracker Green. Figure 4 shows that the fluorescence of that dye with 25  $\mu\text{g/ml}$  saponin remained at control level, thus indicating preservation of the mitochondrial membranes. When the saponin concentration was increased to 50  $\mu\text{g/ml}$ , the fluorescence decreased, yet retaining more than 80% of dye within the mitochondria. Comparison of the fluorescein diacetate and MitoTracker Green signals (Figure 4) shows that the regime of treatment with 50  $\mu\text{g/ml}$  for 15 min was optimum to ensure full permeabilization of the cells, while the intactness of mitochondrial membranes was preserved.

### **Mitochondrial membrane potential**

The potential across the inner mitochondrial membrane plays central role in controlling mitochondrial ATP synthesis,  $\text{Ca}^{2+}$  accumulation and generation of reactive oxygen species. Because each of these factors can influence the viability of the cell, the measuring of  $\Delta\psi\text{m}$  provides important information on the mechanism by which mitochondria influence the survival of the cells. To detect whether the mitochondria are also able to maintain the  $\Delta\psi\text{m}$  after processing with saponin, the saponin-treated neuronal monolayers were incubated with potential-sensitive dye (JC-1), in the absence and in the presence of mitochondrial substrates, 5 mM glutamate and 2 mM malate. After 20 min incubation with JC-1 the fluorescence emission at 522 (DF35) nm and 605 (DF32) nm were detected. Figure 5 ABC shows that stimulation of respiration in mitochondria after addition of respiratory substrates was accompanied by translocation of the JC-1 into mitochondria, as indicated by the increased red fluorescence (Figure 5B) and correspondingly decreased green fluorescence. On the contrary, treatment of cells with FCCP, a mitochondrial uncoupler (1  $\mu\text{M}$ ), led to the disappearance of red fluorescence from mitochondria and enhancement of green fluorescence (Figure 5C). The panels D, E and F in Figure 5 demonstrate that energization and de-energization of mitochondria were associated with reciprocal two-fold changes in red and green fluorescence. Thus, the red to green fluorescence ratio could be taken as an index for monitoring the transitions between the high and low levels of mitochondrial membrane potential, as it changed more than the intensities of the individual fluorescences.

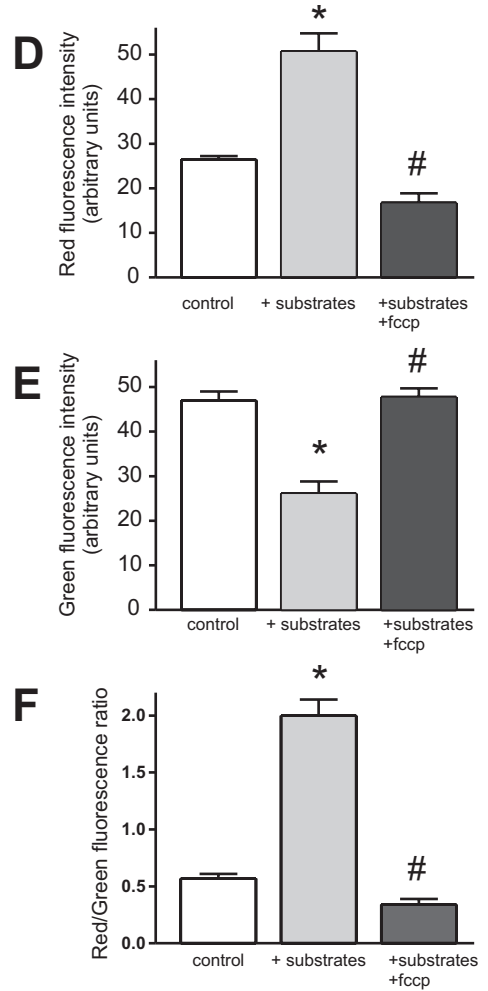
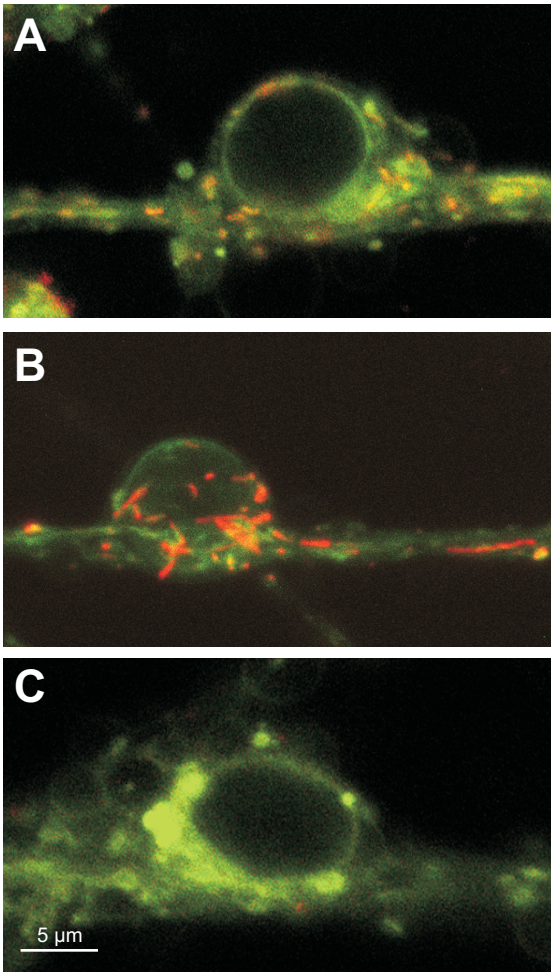


**Figure 5.** JC-1 fluorescence in permeabilized cerebellar granule cells incubated without exogenous substrates (panel A) and with added glutamate and malate in the absence (B) or presence (C) of 1  $\mu$ M FCCP. Panels D, E and F demonstrate the changes in intensities of red and green fluorescence and in their ratio under these conditions, respectively. \* – significantly different from control neurons. # – significantly different from substrate treated neurons. The data are presented as mean  $\pm$  SEM, n = 6–10.



## Measurement of free calcium in mitochondrial matrix

Accumulation of calcium ions into the mitochondria causes great functional consequences for the mitochondria and for the cell both in terms of physiology and pathology. Here we examined mitochondrial calcium sequestration by imaging the fluorescent calcium indicator – fluorinated analogue of rhod-2, acetoxymethyl ester of X-rhod-5F. The acetoxymethyl ester of X-rhod-5F is cationic and membrane-permeant but possesses no detectable calcium-dependent fluorescence. When added to the extra-mitochondrial media, it accumulates in the mitochondria because of the mitochondrial membrane potential. Once de-esterified by mitochondrial esterases, however, X-rhod-5F is retained in the mitochondrial matrix, regardless of mitochondrial membrane potential. Compared with rhod-2 X-rhod-5F has a lower  $\text{Ca}^{2+}$  binding affinity ( $K_d$ : 0.6 and 1.6  $\mu\text{M}$ , respectively) and saturates at higher free  $[\text{Ca}^{2+}]_m$  making it more suitable for monitoring intra-mitochondrial  $\text{Ca}^{2+}$  overload. To verify that X-rhod-5F and its loading protocol led to a specific loading of the mitochondria we carried out control experiments where we also loaded the cells with MitoTracker Green, a mitochondrial specific dye. The results (not shown) indicated that X-rhod-5F and MitoTracker Green were loaded into the same cellular compartment with a characteristic distribution similar to that seen with mitochondrial potential sensitive dye JC-1. To avoid impact of different membrane potentials on loading, all preparations were loaded at high membrane potential after which the experiment was started.

Next, we monitored  $\text{Ca}^{2+}$  accumulation into the mitochondria in condition of calcium overload. Figure 6 A, B and D demonstrate that increase in extramitochondrial  $[\text{Ca}^{2+}]$  from pCa 7.0 to pCa 5.5 was associated with more than 3-fold increase in fluorescence intensity. This accumulation of  $\text{Ca}^{2+}$  was completely abolished by ruthenium red (RR, 10  $\mu\text{M}$ ), a potent inhibitor of  $\text{Ca}^{2+}$  uniporter (Figure 6C, D), whereas no changes were observed in the presence of inhibitors of  $\text{Ca}^{2+}$  efflux, CGP-37157 and cyclosporin A, the inhibitors of mitochondrial  $\text{Na}^+/\text{Ca}^{2+}$  exchanger and permeability transition pore, respectively (results not shown). Thus, the mitochondria gained  $\text{Ca}^{2+}$  exclusively via  $\text{Ca}^{2+}$  uniporter.

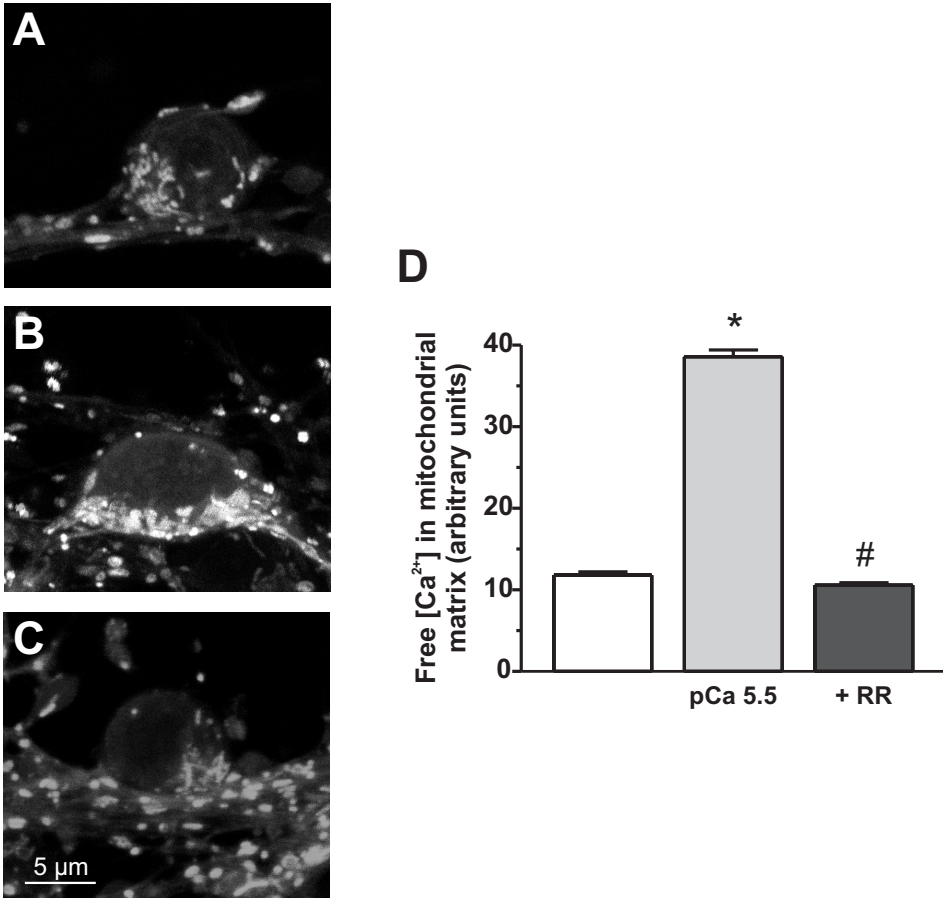


**Figure 6.** X-Rhod-5F fluorescence in permeabilized cerebellar granule cells incubated without exogenous substrates (A) and with added glutamate and malate in the absence (B) or presence (C) of 10  $\mu$ M Ruthenium Red. \* – significantly different from pCa 7.0. # – significantly different from pCa 5.5 treated neurones. The data are presented as mean  $\pm$  SEM, n = 10–12.

### Mitochondrial respiration

Oxygen consumption is one of the most widely used techniques to estimate the functionality of mitochondria. The quality of mitochondrial preparation is most often described by acceptor (ADP) control index, also called respiratory control index (RCI). The RCI is defined as the ratio of the respiration rates of ADP stimulated respiration (referred as state 3) and basal respiration (respiration in the absence of ADP, state 4). Typical RCI values for isolated brain mito-

chondria range from 3 to 7, varying with the substrate applied and the quality of preparation (Wustmann et al., 1987).

Figure 7 and Table 1 demonstrate that the basal respiration (without ADP) of mitochondria in permeabilized cerebellar granule cells was twice higher in case of succinate and nine-fold higher with stimulation of cytochrome oxidase by TMPD and ascorbate compared to that with glutamate/malate substrate pair. Addition of 2 mM ADP stimulated the respiration by 3.9, 5.0 and 1.4 times, in the presence of NADH-linked substrate, FADH<sub>2</sub>-linked substrate and TMPD-ascorbate, respectively. The protocol applied also favors estimation of the activity of cytochrome oxidase that is equivalent to a NaN<sub>3</sub>-sensitive portion of the ADP-stimulated respiration ( $V_{ADP} - V_{NaN_3}$ ). It is thus possible to estimate the functional stoichiometry between the cytochrome oxidase and other complexes of respiratory chain. Notably, the maximal state 3 rate of respiration achieved was similar for both, succinate and TMPD+ascorbate, being more than twice higher than in the presence of glutamate and malate. The same proportions were held for cytochrome oxidase activities. The observation that the cytochrome oxidase activity in the presence of succinate was similar to that in the presence of TMPD, ascorbate suggests that cytochrome c was not detached from the mitochondria during permeabilization of the cells with saponin.

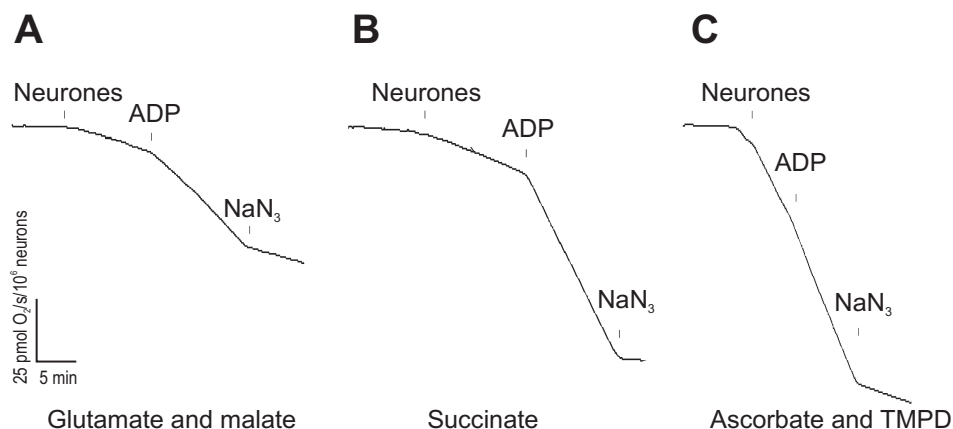


**Figure 7.** Oxygen consumption of permeabilized cerebellar granule cells in the presence of different substrates. (A) 5 mM glutamate plus 2 mM malate; (B) 10 mM succinate and (C) 0.5 mM TMPD plus 2 mM ascorbate. Additions: neurons (5.66·10<sup>6</sup>·ml), 2 mM ADP, and 5 mM NaN<sub>3</sub>.

**Table 1.** Respiratory parameters of permeabilized neurons

|  | <i>Glutamate<br/>and malate</i> | <i>Succinate</i> | <i>TMPD and<br/>ascorbate</i> |
|--|---------------------------------|------------------|-------------------------------|
| $V_0$ (pmolO <sub>2</sub> · s <sup>-1</sup> · 10 <sup>-6</sup> cells)                | 2.3 ± 0.2 (5)                   | 4.2 ± 0.4 (3)*   | 19.3 ± 5.3 (3)**              |
| $V_{ADP}$ (pmolO <sub>2</sub> · s <sup>-1</sup> · 10 <sup>-6</sup> cells)            | 9.0 ± 1.1 (5)                   | 21.0 ± 3.0 (3)** | 24.3 ± 7.1 (3)*               |
| <b>RCI</b>   | 3.9 ± 0.2 (5)                   | 5.0 ± 0.3 (3)*   | 1.4 ± 0.1 (3)***              |
| $V_{NaN3}$ (pmolO <sub>2</sub> · s <sup>-1</sup> · 10 <sup>-6</sup> cells)           | 1.2 ± 0.2 (5)                   | 0.6 ± 0.5 (3)    | 3.1 ± 0.6 (3)                 |
| $V_{ADP} - V_{NaN3}$ (pmolO <sub>2</sub> · s <sup>-1</sup> · 10 <sup>-6</sup> cells) | 7.8 ± 1.4 (5)                   | 20.3 ± 3.5 (3)** | 19.3 ± 6.8 (3)                |

The values are given as mean ± SEM and number of separate experiments is given in parentheses. \*— $p < 0.05$ , \*\*— $p < 0.005$ , \*\*\*— $p < 0.0001$  compared to measurements with glutamate and malate. The concentration of the cells in oxygraph chamber was 5.66 millions per milliliter (50 µg protein/10<sup>6</sup> cells).  $V_0$  – rate of basal respiration;  $V_{ADP}$  – rate of ADP stimulated respiration; RCI – respiratory control index (the ratio of respiration rate in the presence of ADP to that of basal respiration without ADP);  $V_{NaN3}$  – NaN3 insensitive portion of the ADP stimulated respiration;  $V_{ADP} - V_{NaN3}$  – NaN3 sensitive portion of the ADP stimulated respiration.

## The effect of different steroids on neuronal mitochondria in model of ischemia

### Protective effect of different neurosteroids against calcium overload

Next, we employed the method of permeabilization of neuronal cultures to characterize the interactions between neurosteroids and mitochondria.

Ischemia and reperfusion affect mitochondrial function in two ways: oxygen deficiency hampering the respiratory chain and cytoplasmic calcium overload leading to accumulation of Ca<sup>2+</sup> in the mitochondrial matrix. To imitate these mechanisms we treated the skinned neurons either with a respiratory chain inhibitor, 1-methy-4-phenylpyridinium (MPP+) or raised free extra-mitochondrial calcium concentration and detected the ratio of red/green fluorescence of JC-1 after 10 min of incubation. As expected, both applications lowered the red/green fluorescence ratio significantly, indicating a fall of mitochondrial membrane potential. The 50% inhibition was observed at 2mM MPP+ or 2µM free [Ca<sup>2+</sup>].

In the next experiments, the effect of DHEA (100µM, added at the start of incubation with MPP+ or high [Ca<sup>2+</sup>]) against the 5mM MPP+ or 3.2µM free [Ca<sup>2+</sup>] induced loss of mitochondrial potential was studied. In cells treated with MPP+, DHEA had no effect on mitochondrial membrane potential. Cells exposed to high [Ca<sup>2+</sup>] in the presence of DHEA, however, showed significantly higher red to green fluorescence ratio of JC-1 than the ones in absence of DHEA (Figure 8AB).

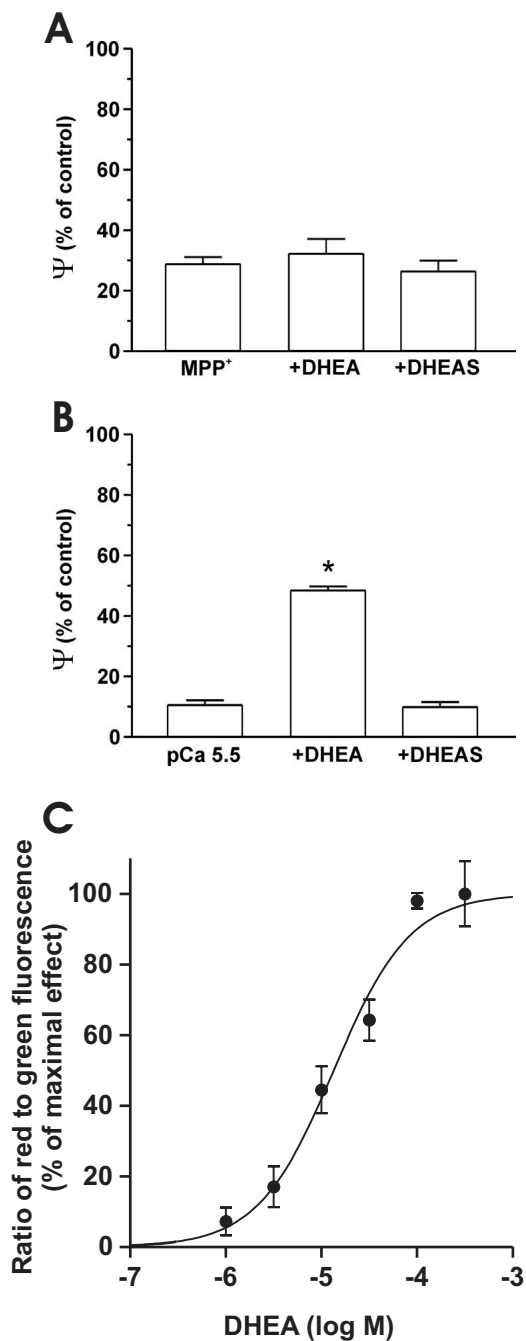


**Figure 8.** Relative  $\Delta\Psi$  measurement using JC-1 in the presence of MPP<sup>+</sup> (5mM, A) or 3.2 $\mu$ M [Ca<sup>2+</sup>] (B); DHEA (100 $\mu$ M) preserved higher red to green fluorescence ratio in the model of Ca<sup>2+</sup> overload (\* – significantly different from pCa 5.5,  $P < 0.05$ ,  $n = 610$ ), but was ineffective against MPP<sup>+</sup>; DHEAS (100 $\mu$ M) was ineffective in both models. JC-1 fluorescence intensities were monitored at 605DF32 and 522DF35nm, relative  $\Delta\Psi$  is expressed % of control JC-1 red/green ratio. (C) Dose response curve of DHEA. Skinned neurons incubated at pCa 5.5 and at different concentrations of DHEA were stained with JC-1. Values are expressed as percentage of maximal effect of DHEA ( $n = 5-8$ ).

The effect of DHEA was concentration dependent. As can be seen from Figure 8C, the maximal response was obtained at 100 $\mu$ M concentration with EC<sub>50</sub> 15 $\mu$ M. A similar effect was observed when the cells were treated with other neurosteroids (100 $\mu$ M) pregnenolone, pregnanolone, allopregnanolone, progesterone and to a lesser extent also 17 $\beta$ -estradiol but not with DHEAS, pregnenolone sulphate or androstenedione (Table 2). 100 $\mu$ M cholesterol was ineffective. It was also tested whether the mixture of neurosteroids in a range of physiological concentrations in the human brain could be protective in this model. As can be seen from Table 2, the mixture of DHEA, DHEAS, pregnenolone, pregnenolone sulfate, and pregnanolone preserved mitochondrial membrane potential in condition of cytoplasmic Ca<sup>2+</sup> overload. It should be noted also that neurosteroids themselves had no effect on the fluorescence spectra of JC-1.

**Table 2.** Effect of different steroids on mitochondrial membrane potential

| <i>Treatment</i>                                | <i>Mean <math>\pm</math> S.E.M.</i> |
|---|-------------------------------------|
| pCa 7.0   | 100 $\pm$ 7                         |
| pCa 5.5   | 36 $\pm$ 2                          |
| pCa 5.5 + DHEA 100 $\mu$ M                      | 63 $\pm$ 7 <sup>a</sup>             |
| pCa 5.5 + DHEAS 100 $\mu$ M                     | 29 $\pm$ 3                          |
| pCa 5.5 + pregnenolone 100 $\mu$ M              | 81 $\pm$ 4 <sup>a</sup>             |
| pCa 5.5 + pregnenolone sulphate 100 $\mu$ M     | 32 $\pm$ 3                          |
| pCa 5.5 + pregnanolone 100 $\mu$ M              | 64 $\pm$ 7 <sup>a</sup>             |
| pCa 5.5 + allopregnanolone 100 $\mu$ M          | 51 $\pm$ 5 <sup>a</sup>             |
| pCa 5.5 + 17 $\beta$ -estradiol 100 $\mu$ M     | 43 $\pm$ 2 <sup>a</sup>             |
| pCa 5.5 + androstendione 100 $\mu$ M            | 40 $\pm$ 5                          |
| pCa 5.5 + cholesterol 100 $\mu$ M               | 38 $\pm$ 2                          |
| pCa 5.5 + mixture of neurosteroids <sup>b</sup> | 50 $\pm$ 2 <sup>a</sup>             |

Relative  $\Delta\Psi_m$  was assessed by monitoring the ratio of JC-1 fluorescence intensities at 605DF32 and 522DF35nm and is expressed as a percentage or control at pCa 7.0.

<sup>a</sup> Difference compared with pCa 5.5 group,  $p < 0.05$ ,  $n = 7-27$

<sup>b</sup> Mixture of neurosteroids contained 150nM DHEA, 200nM DHEAS, 900nM pregnenolone, 100nM pregnenolone sulphate and 4nM pregnanolone.

The effect of DHEA depended on the extra-mitochondrial [Ca<sup>2+</sup>] used. As demonstrated Figure 9, the increasing of external Ca<sup>2+</sup> (up to 32 $\mu$ M of free ion, pCa 4.5) produced a bell-shaped curve: the initial small increase of mitochondrial membrane potential was followed by a decrease when pCa exceeded 6.5. In the presence of 100 $\mu$ M DHEA, however, the initial rise was significantly higher and the whole curve for membrane potential was shifted to the right. Thus, while in control preparations the membrane potential fell to half of the

initial value at pCa 5.7 (2 $\mu$ M), the same level (50% of control value) was achieved significantly later, at pCa 5.3 (5 $\mu$ M) in the DHEA treated group.

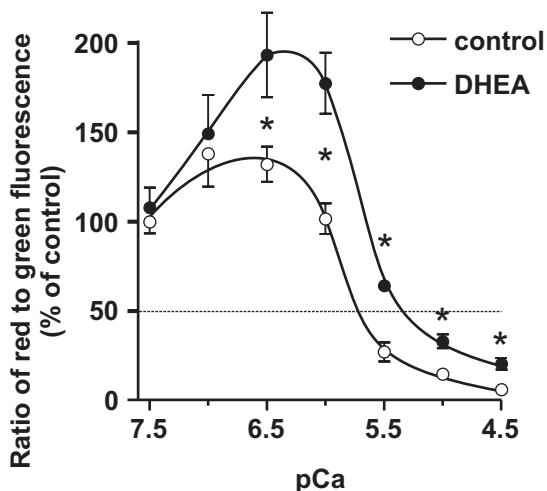


**Figure 9.** Effect of DHEA on mitochondrial membrane potential at different free Ca<sup>2+</sup> concentrations. Skinned neurons incubated at different free Ca<sup>2+</sup> concentrations in the presence or absence of 100  $\mu$ M DHEA were stained with JC-1. Relative  $\Delta\Psi$  was assessed by monitoring the ratio of JC-1 fluorescence intensities at 605DF32 and 522DF35 nm and is expressed as a percentage of control at pCa 7.5. Asterisk signifies difference between groups,  $P < 0.05$ ,  $n = 6-14$ .

It should be noted here that a similar shift, however, more potent, was observed in the presence of the inhibitor of mitochondrial Ca<sup>2+</sup> influx, ruthenium red, e.g. 10 $\mu$ M ruthenium red led to an increase in membrane potential at pCa 7.0 and was also protective at higher Ca concentrations between pCa 5.5 and 4.5. At the same time CGP-37157 or cyclosporin A, inhibitors of mitochondrial Ca<sup>2+</sup> efflux pathways, did not reverse the protective effect of DHEA. Both compounds alone had no effect on membrane potential suggesting that DHEA do not activate the Ca<sup>2+</sup> efflux pathways but rather inhibit the influx of Ca<sup>2+</sup> into the mitochondrial matrix.

### DHEA effects on mitochondrial calcium accumulation

To determine whether the effects of DHEA on mitochondrial membrane potential are associated with intramitochondrial [Ca<sup>2+</sup>] we carried out experiments to directly measure free [Ca<sup>2+</sup>] in the mitochondrial matrix.

First, we measured the X-rhod-5F response following the increase in extra-mitochondrial [Ca<sup>2+</sup>] up to pCa 5.5 in the presence of Ca efflux inhibitors, CGP-

37157 and cyclosporin. The calcium accumulation was partially inhibited in the presence of 100 $\mu$ M DHEA. For quantitative analysis, the mean intensity of X-rhod-5F fluorescence was determined in 8–20 random microscopy fields (200–300 neurons per field). The results show that high extra-mitochondrial [ $\text{Ca}^{2+}$ ] led to a three-fold increase of fluorescence intensity over the control values from which 30% was reduced by DHEA (Figure 10).

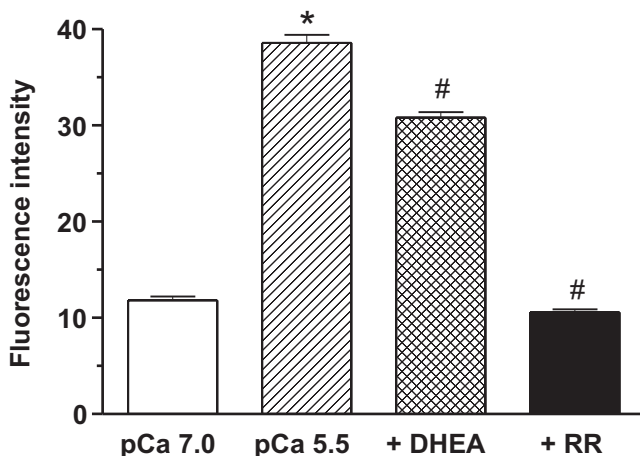


**Figure 10.** Measurement of free [ $\text{Ca}^{2+}$ ] in the mitochondrial matrix. Skinned neurons stained with X-Rhod-5F-AM were incubated at pCa 7.0 as a control or at pCa 5.5 in the absence or presence of 100  $\mu$ M DHEA or 30  $\mu$ M Ruthenium Red. All experiments were performed in the presence of 10 $\mu$ M CGP-37157 and 10  $\mu$ M cyclosporin to block the mitochondrial  $\text{Ca}^{2+}$  efflux pathways. Relative free [ $\text{Ca}^{2+}$ ] in the mitochondrial matrix was assessed by monitoring the X-Rhod-5F fluorescence intensity at 605DF32 nm. Asterisk indicates significant difference vs. control and cross vs. pCa 5.5,  $P < 0.01$ ,  $n = 8-20$ .

Similar results were obtained when isolated mitochondria were used. Mitochondria were loaded with X-Rhod-5F, incubated at different pCa for 20min and after that the intra-mitochondrial free  $\text{Ca}^{2+}$  was detected. In this case, treatment with DHEA at the same concentration as in situ experiments (100 $\mu$ M) lowered significantly the sensitivity of mitochondrial  $\text{Ca}^{2+}$  accumulation to extra-mitochondrial [ $\text{Ca}^{2+}$ ] (from  $0.5 \pm 0.1$  to  $0.9 \pm 0.2 \mu\text{M}$ ,  $P < 0.01$ ) without affecting the maximal  $\text{Ca}^{2+}$  concentration in the matrix (not shown). From these results we conclude that DHEA inhibits partly the  $\text{Ca}^{2+}$  influx into the mitochondrial matrix.



# Regulation of mitochondrial shape in cultured neurons

## Regulation of mitochondrial volume

Mitochondrial membrane potential causes the ions of opposite sign of charge to leak through the inner mitochondrial membrane, which are extruded from mitochondria in order to prevent swelling and lysis. Thus, dynamic regulation of mitochondrial ion flux, particularly potassium flux, is essential for structural and functional integrity of mitochondria. Still, several major questions concerning the mechanisms, extent and relevance of mitochondrial volume regulation have remained unanswered. Until now further research in that direction has been significantly impeded through lack of the adequate methodology allowing us to study the mitochondrial volume in their natural cellular environment.

Using the deconvolution confocal microscopy we quantified the volume as well of other morphological parameters of single neuronal mitochondrion in permeabilized culture of cerebellar granule cells. Figure 11A shows typical surface rendered reconstruction of 3D data sets of mitochondria in situ in control conditions. Mitochondria appear rod-shaped with an average length of  $2294 \pm 104$  nm and with an average diameter in focal plane of  $207 \pm 6$  nm (determined from 42 mitochondria from 42 different preparations). Diameter measured along the optical axis (z axis) was smaller,  $155 \pm 9$  nm.

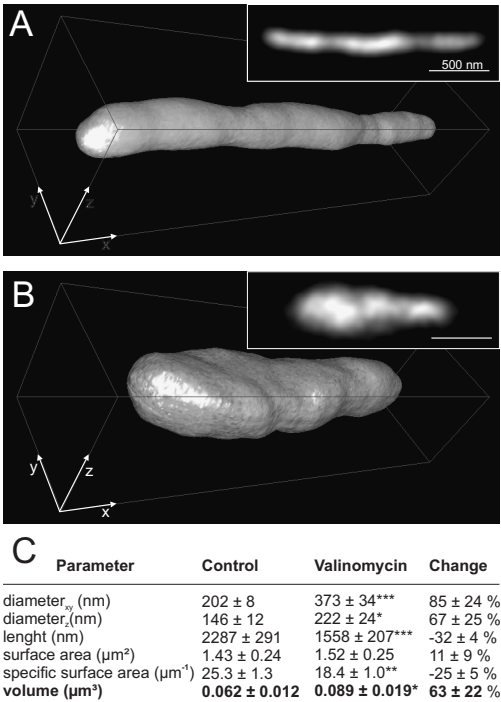


**Figure 11.** Isosurface 3D reconstruction of a MitoTracker Green stained mitochondrion in permeabilized neuron before (A) and 5 min after (B) treatment with 10  $\mu$ M valinomycin (frame size 2250 x 500 x 500 nm). Inserts depict the XY maximal projections of respective images series. Panel C depicts the morphological parameters of 11 mitochondria before (control) and after valinomycin treatment, and gives the mean change from control values. \*  $p < 0.05$ , \*\*  $p < 0.01$  and \*\*\*  $p < 0.001$

### The effect of potassium ionophore valinomycin

Our next step was to estimate remodeling of the mitochondrial morphology in response to various stimuli modulating transmembrane potassium flux. First, the mitochondria were incubated with 10  $\mu\text{M}$  valinomycin, which acts as a mobile carrier ensuring the potential-driven net potassium uptake thus inducing the mitochondrial swelling. In our preparation, treatment with valinomycin led to a fast response in mitochondrial morphology within minute – the mitochondrion that was initially thread-like in structure became notably rounded. Three-D reconstructions of the same mitochondrion before and after valinomycin treatment clearly demonstrate that shortening of the mitochondrion was accompanied with its thickening both in optical plane and along the optical axis (Figure 11B). Morphometric analysis (Figure 11C) shows that observed shortening of mitochondria was not associated with any considerable change in mitochondrial surface area. However, it was characterized by a statistically significant 1.6-fold increase in the mitochondrial volume. Similar, a 1.75-fold increase was observed also for the specific surface area (ratio between surface area and volume) indicating change in morphology.

### The effect of $K_{\text{ATP}}$ -channel opener pinacidil

Similar changes were observed when mitochondria were exposed to an ATP-sensitive  $K^+$  channel opener, 100  $\mu\text{M}$  pinacidil (Figure 12). It should be noted, however, that in contrast to the response to valinomycin where the swelling was uniform, different subpopulations of mitochondria tended to respond differently to pinacidil. As shows Figure 12, some of the mitochondria become notably rounded when others shortened just slightly. Another feature of the pinacidil response was the transient nature of swelling. Some of the mitochondria tended to restore their original shape after initial swelling. It is important to note here that when compared with treatment with valinomycin collapsing the membrane potential, mitochondrial membrane potential was still relatively high in pinacidil-treated mitochondria even in case of swelling (Figure 13C).

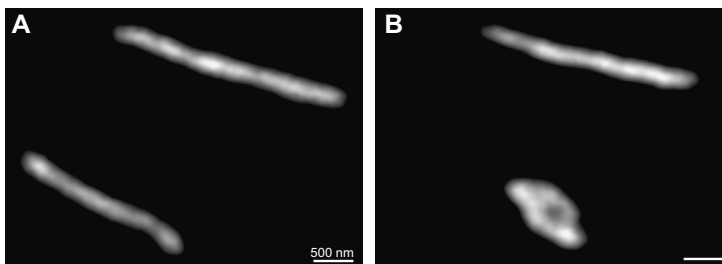


**Figure 12.** Effect of 100  $\mu\text{M}$  pinacidil on mitochondrial morphology in permeabilized neurons. Panel A – mitochondria in control conditions, panel B – the same mitochondria after pinacidil treatment.

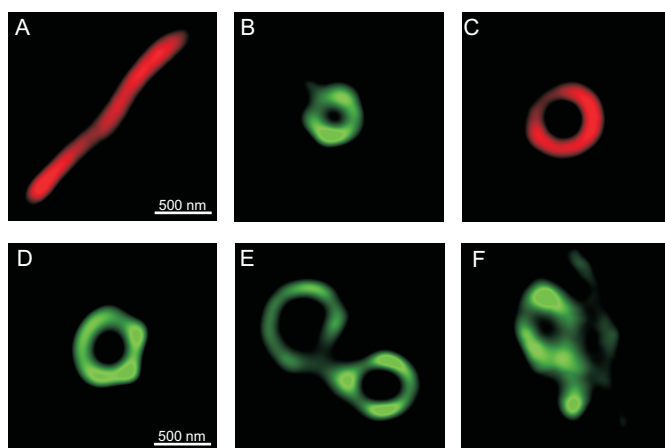


**Figure 13.** Visualization of mitochondrial membrane potential by JC-1 in control (A) and with 10  $\mu$ M valinomycin (B), 100  $\mu$ M pinacidil (C), 20  $\mu$ M FCCP plus 50  $\mu$ M oligomycin (D), 25 mM azide (E) or 100  $\mu$ M antimycin plus 50  $\mu$ M oligomycin (F) treated permeabilized neurons (green, emission at 522DF35 nm – low potential; red, emission at 605DF32 nm high – potential).

### The effect of inhibitor of K/H exchanger

When the mitochondria were exposed to 500  $\mu\text{M}$  propranolol inhibiting mitochondrial  $\text{K}^+/\text{H}^+$  exchanger, the swelling was very fast and within minutes the mitochondria seemed to loose their membrane integrity and lost the mitochondrial marker. Only few mitochondria remained intact after 5 minute treatment with propranolol (Figure 14).

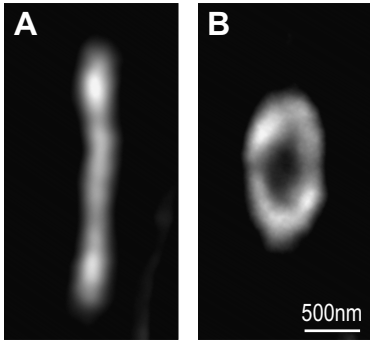


**Figure 14.** Effect of 500  $\mu\text{M}$  propranolol on mitochondrial morphology in permeabilized neuron. Panel A shows the mitochondria in control conditions and panel B the same mitochondria after propranolol treatment.

### The effect of uncoupling

We next examined the effects of the mitochondrial uncoupler FCCP, which rapidly dissipated the mitochondrial membrane potential. Figure 15B demonstrates that treatment with 20  $\mu\text{M}$  FCCP in the presence of leads to similar changes in mitochondrial morphology as valinomycin does. After 5 min treatment with FCCP, mitochondria become shorter and their width in focal plane and thickness in optical axis increased significantly (Table 3). These changes in mitochondrial morphology were also associated with a significant 1.75 fold increase in volume without marked changes in mitochondrial surface area. Similar results were obtained when mitochondria were treated with FCCP in the presence of 50  $\mu\text{M}$  oligomycin. Figure 13D confirms that under our treatment conditions, the mitochondrial membrane potential was indeed collapsed after FCCP treatment.

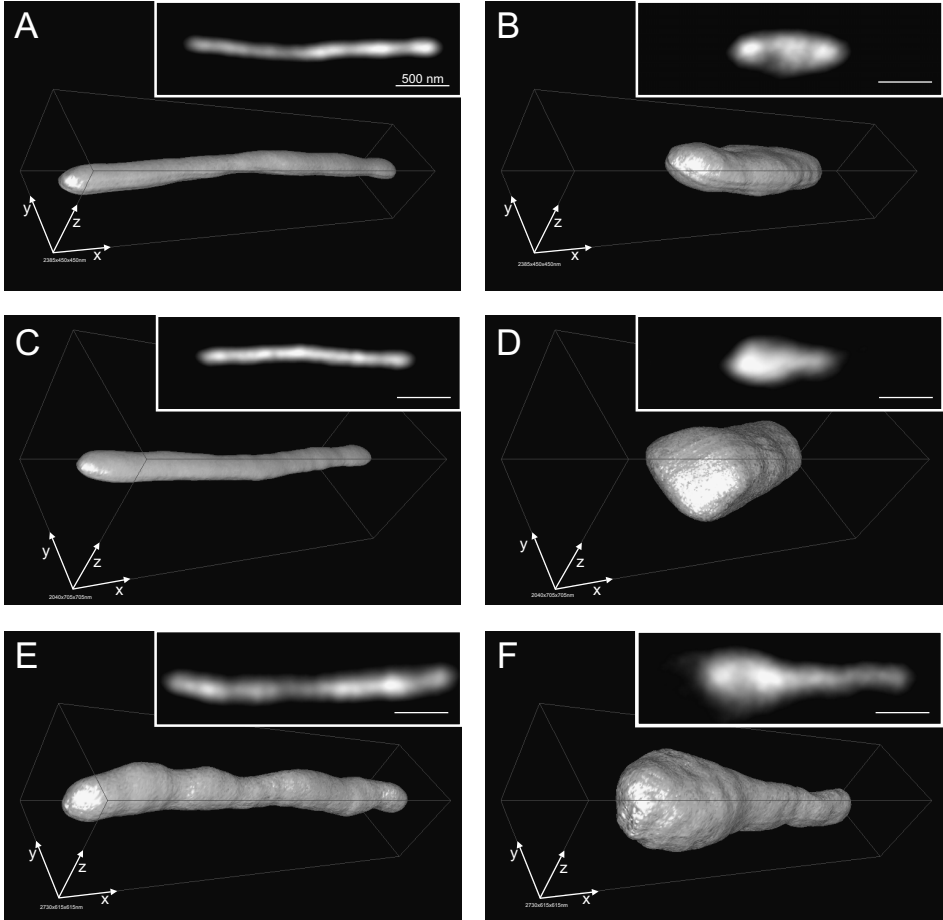


**Figure 15.** Isosurface 3D reconstruction of a MitoTracker Green stained mitochondrion in permeabilized neuron before (A, C, E) and 5 min after treatment with 20  $\mu$ M FCCP plus 50  $\mu$ M oligomycin (B; frame size 2385 x 450 x 450 nm) or 25 mM azide (D; frame size 2040 x 750 x 750 nm) or 30 min after treatment 100  $\mu$ M antimycin plus 50  $\mu$ M oligomycin (F; frame size 2730 x 615 x 615 nm). Inserts depict the XY maximal projections of respective image series.

**Table 3.** Morphological parameters of mitochondria

| <b>FCCP (n=10)</b>                        | <b>Control</b>       | <b>Treatment</b>       | <b>Change</b>     |
|---|----------------------|------------------------|-------------------|
| diameter <sub>xy</sub> (nm)               | 215 ± 13             | 386 ± 49*              | 89 ± 31 %         |
| diameter <sub>z</sub> (nm)                | 176 ± 16             | 291 ± 29**             | 76 ± 22 %         |
| length (nm)                               | 2286 ± 166           | 1575 ± 142**           | -30 ± 5 %         |
| surface area (μm <sup>2</sup> )           | 1.43 ± 0.13          | 1.57 ± 0.15            | 14 ± 11 %         |
| specific surface area (μm <sup>-1</sup> ) | 24.6 ± 1.9           | 17.3 ± 1.1**           | -27 ± 6 %         |
| <b>volume (μm<sup>3</sup>)</b>            | <b>0.063 ± 0.008</b> | <b>0.098 ± 0.015*</b>  | <b>75 ± 22 %</b>  |
| <b>AZIDE (n=10)</b>                       | <b>Control</b>       | <b>Treatment</b>       | <b>Change</b>     |
| diameter <sub>xy</sub> (nm)               | 203 ± 11             | 460 ± 49***            | 129 ± 23 %        |
| diameter <sub>z</sub> (nm)                | 140 ± 15             | 240 ± 39*              | 93 ± 47 %         |
| length (nm)                               | 2180 ± 168           | 1252 ± 114***          | -41 ± 5 %         |
| surface area (μm <sup>2</sup> )           | 1.16 ± 0.11          | 1.48 ± 0.21            | 32 ± 15 %         |
| specific surface area (μm <sup>-1</sup> ) | 27.9 ± 1.8           | 17.2 ± 1.1**           | -37 ± 4 %         |
| <b>volume (μm<sup>3</sup>)</b>            | <b>0.045 ± 0.006</b> | <b>0.095 ± 0.019*</b>  | <b>133 ± 45 %</b> |
| <b>ANTIMYCIN (n=9)</b>                    | <b>Control</b>       | <b>Treatment</b>       | <b>Change</b>     |
| diameter <sub>xy</sub> (nm)               | 213 ± 9              | 454 ± 48***            | 124 ± 26 %        |
| diameter <sub>z</sub> (nm)                | 149 ± 20             | 261 ± 43*              | 94 ± 39 %         |
| length (nm)                               | 2416 ± 198           | 1628 ± 210*            | -32 ± 7 %         |
| surface area (μm <sup>2</sup> )           | 1.53 ± 0.19          | 1.78 ± 0.19            | 23 ± 20 %         |
| specific surface area (μm <sup>-1</sup> ) | 27.1 ± 3.1           | 18.2 ± 2.4*            | -29 ± 8 %         |
| <b>volume (μm<sup>3</sup>)</b>            | <b>0.067 ± 0.011</b> | <b>0.1113 ± 0.017*</b> | <b>139 ± 76 %</b> |

Comparisons of morphological parameters of mitochondria in permeabilized neurons before and after treatment with FCCP (20 μM + 50 μM oligomycin), 25 azide (mM) or antimycin (100 μM + 50 μM oligomycin). Parameters were measured from isosurface 3D reconstructions of the MitoTracker Green stained mitochondria. Change – mean change from predrug (control) values. \* p<0.05, \*\* p<0.01 and \*\*\* p<0.001.

### The effect of inhibition of respiratory chain

Next, we tested the effects of two inhibitors of respiratory chain, antimycin and sodium azide, inhibiting respectively succinate-ubiquinone reductase and cytochrome c oxidase. In case of antimycin also oligomycin was added to prevent the potential reverse activity of mitochondrial ATP synthetase. In control experiments where oligomycin was added alone, no change in mitochondrial morphology was detected. Oligomycin was not added in case of azide as the latter have been shown to inhibit ATP synthase itself (Vasilyeva et al., 1982; Muneyuki et al., 1993). Figures 13 and 15 demonstrate that similarly to FCCP, 30 min treatment with antimycin plus oligomycin or 5 min treatment with azide

collapsed the mitochondrial membrane potential and induced evident changes in mitochondrial morphology. As seen in the Table 3, both treatments led to more than 2 fold increase in the mitochondrial volume with slight and statistically insignificant increase in mitochondrial surface areas.

To check whether these effects of uncoupling and respiratory chain inhibition are related to potassium flux, we performed similar experiments also in the absence of potassium, in sucrose media. Under these conditions, treatment with FCCP or azide had no effect on mitochondrial morphology (results not shown).

To exclude the possibility that observed effects are artifacts present only in our artificial conditions (plasma membrane permeabilized cells, specific milieu, room temperature), we tested also the effect of FCCP and azide in intact neurons in their cell culture media at 37°C. The results demonstrated that changes observed in permeabilized preparations were present also, and even more visibly, in intact preparations (Figure 16).

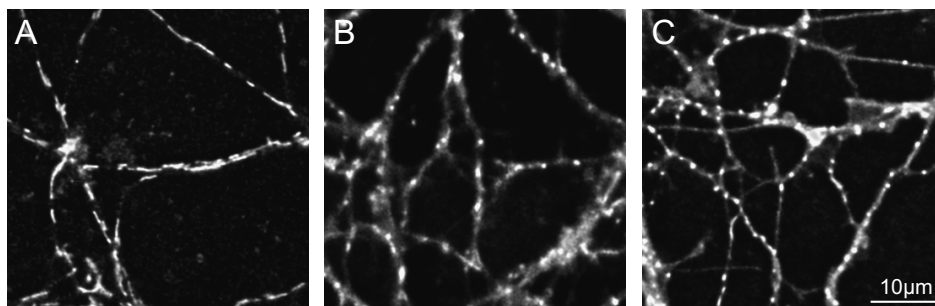


**Figure 16.** Effect of FCCP and azide on mitochondrial morphology in intact neurons in their cell culture media at 37°C. Panel A shows the mitochondria in control conditions and panels B and C after treatment with 20  $\mu$ M FCCP and 25 mM azide, respectively.

### **Changes in mitochondrial volume affect the transport of mitochondria in neurons**

The next important question was whether such a remodeling of mitochondrial morphology could affect dynamic behavior of mitochondria in neurites. We tracked the motility of single mitochondria under control conditions during 5 minutes. Analysis of the track data shows that as an average the mitochondria spent  $65 \pm 2\%$  ( $n=120$ ) of time in motile state. Average mitochondrial velocity during measurement period was  $0.19 \pm 0.01 \mu\text{m/s}$  (range 0–0.62  $\mu\text{m/s}$  with median 0.16  $\mu\text{m/s}$  and mood 0.23  $\mu\text{m/s}$ ,  $n=120$ ). However, treatment with different swelling-inducing agents like valinomycin, FCCP and azide, lead to immediate and complete cessation of mitochondrial traffic. As demonstrates Figure 17, the mitochondria lost almost completely their motility and remained

in stationary most of the time and as well the average velocity of these mitochondria during measurement period that included both stationary and motile states dropped more than 20-fold.

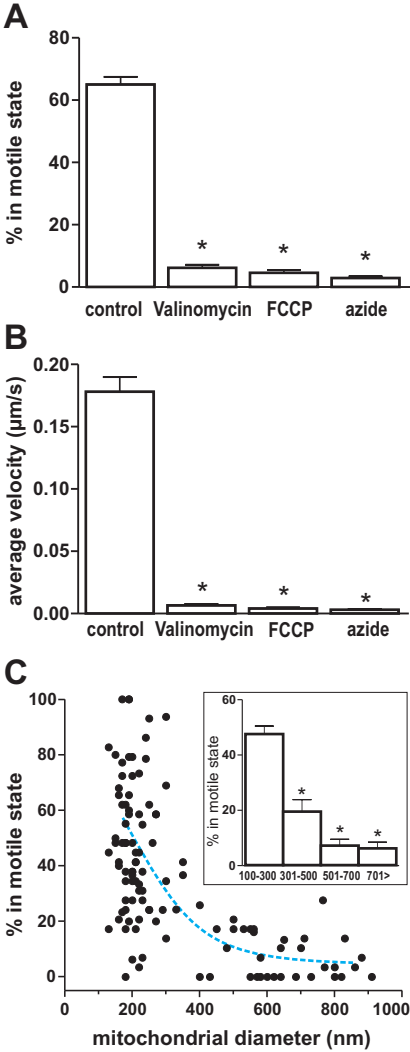


**Figure 17.** Effect of valinomycin (10  $\mu\text{M}$ ), FCCP (20  $\mu\text{M}$ ) and azide (25 mM) on mitochondrial motility in intact neurons as measured by percentage of mitochondria in motile state (A) or average velocity (B). Panel C shows the correlation between mitochondrial diameter and motility in the presence of pinacidil. Insert depicts the same correlation as a bar-graph.

However, mitochondrial traffic is energy dependent process and valinomycin, FCCP or azide are disrupting the mitochondrial membrane potential affecting energy supply. Observed changes could be thus related to energy failure of neurons rather than to the mitochondrial morphology. To differentiate between these two options, we took an advantage of heterogeneous effect of the pinacidil and the fact that pinacidil is not disrupting the mitochondrial membrane potential even in swollen mitochondria (see Figure 13). Effect of pinacidil was



heterogeneous also in intact neurons e.g. part of the mitochondria begun to swell while another part remained unchanged. We then measured the diameter of mitochondria from 2D deconvoluted images and tracked the motion of each of these mitochondria. Results of these measurements plotted in Figure 17C show clear relationship between diameter and motility: mitochondria with higher diameter were mostly in stationary state while mitochondria with lower, normal diameter kept moving. It should be also remarked here that this process was reversible. Swollen stationary mitochondria become sometime motile after they restored their normal rod shape morphology. These results show clearly that mitochondria morphology could be one of the factors controlling mitochondrial traffic.

### **Reconstruction of mitochondria in neuronal processes and their colocalization with cytoskeleton**

We can provide two explanations how this could be happen. First, the increase in mitochondrial diameter could mechanically hamper the mitochondrial passage in narrow neurites. We stained the cytoplasm in neurites with Cell Tracker Green and measured the diameter of cytoplasm in neurites from 3D reconstructions of these images. Mean diameter of cytoplasm in neurites, measured in focal plane, was  $294 \pm 18$  nm ( $n=21$ , range 164–500) and thus at the same range with mitochondrial diameter ( $207 \pm 6$  nm) at control conditions visualized in Figure 18A. In the presence of agents used to induce mitochondrial swelling no change in diameter of neurites was observed while mitochondrial diameter increased considerably (Figure 18B).

Another option could be that increased mitochondrial roundness could decrease the number of potential contact sites between microtubules and mitochondria for motor proteins. In Figure 18CD, where paclitaxel (Taxol) conjugated to Oregon Green was used to visualize tubulin and MitoTracker Red for mitochondria, shows that the contact between mitochondria and myofilaments is decreased indeed. These result suggest that both options, increased mitochondrial diameter exposing mechanical constraints and increased roundness decreasing the contact sites with neurofilaments could be related with decreased motility of swollen mitochondria.

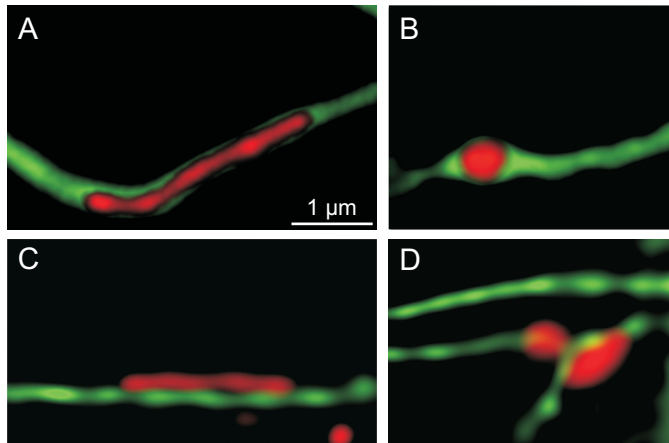


**Figure 18.** Visualization of mitochondria by MitoTracker Red with cytoplasm (A and B; stained by CellTracker Green) or microtubules (C and D: stained by paclitaxel conjugated to Oregon Green) in intact neurons. Panels A and C – control, panels B and C swollen mitochondria in the presence of 100  $\mu$ M pinacidil. In panels A and B the red channel is superimposed to the green channel to improve visualization of mitochondria in neurites. Note also that microtubules in panels C and D appear considerably thicker since the deconvolution process could not fully restore such thin structures.

## DISCUSSION

### Measurement of mitochondrial function in situ in permeabilized neuronal cultures

Understanding the role and mechanisms of the involvement of mitochondria in neuronal diseases is of principal importance for elaborating the optimal therapeutic strategies. Studies of neuronal mitochondria, however, have been limited mostly to the use of purified preparations of mitochondria, homogenates or living neurons or neuronal tissues. All these methods have serious drawbacks (either the mitochondria become damaged or affected by cytoplasmic processes) and does not allow to study the function of neuronal mitochondria in their natural milieu e.g. in cells but without influence of cytoplasmic factors. Here we demonstrate that the neuronal cell's membrane can be effectively permeabilized by saponin-treatment and that the permeabilized neurons could be used for qualitative and quantitative assessments of mitochondrial functions, such as oxygen consumption in combination of mitochondrial membrane potential and free calcium in the matrix.

First our results show that the mitochondrial membrane potential in permeabilized neurons was effectively controlled by substrates and uncoupler that was demonstrated by using the ratiometric fluorescence dye JC-1. In our experiments, application of respiratory substrates was associated with the increased red fluorescence in the mitochondria, this suggesting reaching of  $\Delta\psi_m$  above 100 mV, whereas FCCP effectively abolished this change. This effective buildup of membrane potential would have been impossible were the mitochondrial inner membrane impaired.

Second, our results show that the mitochondrial inner membrane preserved its property to effectively control the  $\Delta\psi_m$ -dependent accumulation of  $\text{Ca}^{2+}$  into the matrix in case of cytoplasmic  $\text{Ca}^{2+}$  overload, that could not be detected when inner mitochondrial membrane is permeabilized.

Third, the respiration of mitochondria was effectively controlled by different respiratory substrates and ADP in saponin-permeabilized neurons. In our experiments the proton leak (the basal respiration rate) increased in response to different substrates according to the following order glutamate/malate < succinate < TMPD+ascorbate. These substrate-specific differences of non-phosphorylating respiration can be attributed to different number of the sites of coupling of electron flow to the  $\text{H}^+$  pump, i.e. 3, 2 and 1, in the presence of glutamate/malate, succinate, and TMPD+ascorbate, respectively (Guérin, 1991). When the oxidative phosphorylation was induced by the addition of ADP (state 3), the highest rates of respiration were registered in the presence of TMPD+ascorbate and succinate, whereas the lowest rate was observed in the presence of glutamate/malate. These results suggest that respiration rates with NAD-linked substrates are limited at the level of the complex I or upstream and

may not truly reflect the oxidative capacity of mitochondria. Mitochondrial studies in permeabilized neurons (or isolated neuronal mitochondria) should thus include measurements of respiration rates supported both by NADH and FADH linked substrates. In case when only one substrate should be used then succinate should be preferred as it gives higher respiratory values and better RCI.

## **Effect of neurosteroids on mitochondrial function**

Many evidences indicate that mitochondrial dysfunctions play an important role in the pathophysiologic mechanisms of acute neurodegeneration caused by ischemia. Cytoplasmic  $\text{Ca}^{2+}$  overload and subsequent  $\text{Ca}^{2+}$  accumulation in the mitochondrial matrix are among the most devastating events of ischemic damage. Resultant loss of mitochondrial membrane potential and the concomitant decline in energy production are associated with the increased open probability of the mitochondrial permeability pore. Opening of the latter is a catastrophic event leading to the “death” of mitochondrion that will initiate pathways to cell death (Leist and Nicotera, 1998; Nicholls and Budd, 2000). Thus, any compound that could block the mitochondrial  $\text{Ca}^{2+}$  influx reducing thus the mitochondrial  $[\text{Ca}^{2+}]$ , preserves the mitochondrial membrane potential and thereby protects cells from the initiation of death cascades.

The present study demonstrates that DHEA and as well the other neurosteroids inhibit  $\text{Ca}^{2+}$  influx into the mitochondria. The mitochondrial calcium uptake pathway is electrogenic and is expected to cause a depolarization of the mitochondrial potential. Inhibition of  $\text{Ca}^{2+}$  influx, on the other hand, should have an opposite effect and support the mitochondrial membrane potential. Indeed in the presence of DHEA, suggested to inhibit that pathway, and at free  $\text{Ca}^{2+}$  concentrations higher than  $0.32\mu\text{M}$ , the mitochondrial membrane potential was always higher than in the control group. On the other hand, the effect of DHEA either on membrane potential or  $\text{Ca}^{2+}$  accumulation was not modulated by the inhibitors of mitochondrial  $\text{Ca}^{2+}$  efflux pathways suggesting that the observed effect was due because of inhibiting the influx and not because of the activating of efflux pathways. Moreover, the observed effect of DHEA was also evident at conditions of  $\text{Ca}^{2+}$  overload (at  $\text{pCa } 6-5$ ). The latter allows the suggestion that in the presence of DHEA the mitochondria could be more resistant to cytoplasmic  $\text{Ca}^{2+}$  overload.

In our experiments, the protective effect of DHEA became evident at micromolar concentrations and achieved 50% level at  $15\mu\text{M}$  concentration. This is in the same range as observed in some in vitro experiments showing that DHEA protects hippocampal cells or hippocampal neurons against oxidative stress or excitotoxic damage at  $\mu\text{M}$  concentrations (Bastianetto et al., 1999; Cardounel et al., 1999). Blood levels of DHEA(S) range within  $1-10\mu\text{M}$  but

only a very small fraction of it circulates as free steroid (Baulieu et al., 1998, 2000). Although the free form dominates in the brain, its concentration does not reach micromolar levels (Bixo et al., 1997). This makes it unlikely that DHEA alone could affect the mitochondrial  $\text{Ca}^{2+}$  homeostasis in physiological conditions. However, our finding, that also other neurosteroids, pregnenolone, pregnanolone, allopregnanolone and also estradiol had a similar effect, suggests this effect to be not specific to DHEA but rather to several neurosteroids. Structural requirements for steroid interaction with the mitochondria seem to involve  $\alpha$ -hydroxyl at C3 of the steroid A ring. At the same time, cholesterol alone was ineffective suggesting that the above-mentioned effect is not common for all steroid structures.

Considering that the concentration of free neurosteroids is much higher in the brain than in blood and reaching to the micromolar level (Weill-Engerer et al., 2002; Bixo et al., 1995; Lacroix et al., 1987), it cannot be excluded that the pool of endogenous neurosteroids in the brain acts as a gatekeeper for mitochondrial  $\text{Ca}^{2+}$  influx, regulating thus the mitochondrial response to cytoplasmic  $\text{Ca}^{2+}$  overload. This is supported by our results showing that the mixture of neurosteroids at concentration range observed in the human brain (Weill-Engerer et al., 2002) protected mitochondrial membrane potential from cytoplasmic  $\text{Ca}^{2+}$  overload.

## **Regulation of mitochondrial volume and its physiological role in neurons**

Mitochondrial volume homeostasis is essential for maintaining the structural integrity of the organelle and is one of the factors controlling electron transport, ROS production and the release of apoptotic factors by mitochondria. However, several major questions remain concerning the mechanisms, extent and relevance of mitochondrial volume regulation. Until now, research in that direction has been impeded due to the lack of techniques for studying mitochondrial volume in their natural cellular environment. When using fluorescence microscopy, the diffraction limit restricts resolution of objects smaller than  $\sim 250$  nm (for green light) and because of diffraction caused blur mitochondria with actual diameter around 200 nm appear in these images considerably thicker (400–500 nm) than they are. Moreover, as the blur depends on object roundness, the thin rod-like structures appear considerably more enlarged than spherical objects. It is therefore difficult if not impossible to conclude in what extent and even in what direction the mitochondrial volume changes. This could explain also the ambiguity of previous studies where decreased mitochondrial length has been related with both decreased mitochondrial size (Rintoul et al., 2003) and increased mitochondrial volume (Kahlert and Reiser, 2002).

However, properly calibrated 3-D deconvolution analysis used by us allows to remove diffraction-induced blur and to visualize mitochondrion in its actual size. Volume measurements based on 3D reconstructions of these deblurred images show that described transition from rod-shape to spherical morphology could be associated with more than two-fold increase in mitochondrial volume. These observations demonstrate that changes in mitochondrial volume could be much more substantial as suggested before and not limited to 10–20 percents (Das et al., 2003). It is important to note that even when the mitochondrial volume increases more than 2-fold the surface area is not increasing significantly.

Our results also demonstrate very clearly that mitochondrial depolarization increases the mitochondrial volume. Treatment either with uncoupler or different respiratory chain inhibitors led to obvious remodeling of mitochondrial morphology accompanied with 75–150% increase in mitochondrial volume. Similar results showing that mitochondrial uncoupler induces mitochondrial shortening and increased roundness has been published before but they lack the numerical data of mitochondrial volume (Gao et al., 2001; Minamikawa et al., 1999; Lyamzaev et al., 2004). It should be marked, however, that two other reports failed to demonstrate significant change in mitochondrial morphology in response to uncoupler (Rintoul et al., 2003; Kahlert and Reiser, 2002). One major limitation of previous studies done in living cells is that it was difficult to discriminate the primarily occurring mitochondrial events from those secondarily caused by cellular dysfunction and initial events of cell death. Here we used plasma membrane permeabilized neurons to ensure that all observed events are primarily mitochondrial.

What could be the mechanism underlying the observed swelling? Mitochondrial steady-state volume reflects a zero net flux balance between  $K^+$  influx and  $K^+$  efflux via the mitochondrial  $K^+/H^+$  antiporter. Although, it has been suggested that the balance of  $K^+$  fluxes is shifted toward influx (last reviewed by Garlid and Paucek, 2003), an opposite possibility cannot be excluded. Potassium extrusion in energized mitochondria may overbalance the influx keeping mitochondria contracted. On the contrary, in deenergized mitochondria where extrusion pathway becomes inhibited, the potassium influx could exceed its extrusion. Although indirectly, our results will suggest that the last possibility is applied in neurons. If this model is correct, then the contribution of the exchanger is more important than influx as loss of membrane potential inhibits also the flux directed to the matrix. This hypothesis is supported by our finding that propranolol inhibiting the  $K^+/H^+$  antiporter induces dramatic mitochondrial swelling.

Increase of mitochondrial volume in response to decreased mitochondrial potential may meet different needs and will give the answer to several currently opened questions: First, it is suggested that increase in matrix volume will activate the respiratory chain, providing more ATP to support the cell (Halestrap, 1989; Grover and Garlid, 2000; O'Rourke, 2000). When the need for ATP is high and mitochondria are synthesizing ATP at very high rates then  $\Delta\psi_m$

decreases. If depolarization induced the mitochondrial contraction (as proposed by Garlid and Paucek, 2003) this would favor a decline in ATP production being a bizarre regulatory mechanism. Our results, however, evidence more logically that energetic stress followed by a decrease in  $\Delta\psi_m$  could be associated with increase in matrix volume and thus activate further the respiratory chain.

Second, mitochondrial swelling is associated with ischemic and apoptotic cell death. Recent work by Gogvadze et al. (2004) suggests that one of the key events of the cell death, release of cytochrome c, could be actually triggered by increased in mitochondrial volume. Under these circumstances it is hard to believe that respiring mitochondria are continuously in semi-swollen state and contract in ischemic conditions when potential decreases. Current results suggesting that actively respiring mitochondria remain in contracted and ischemic mitochondria in swollen state suit more with that hypothesis.

Third, our results suggest that mitochondrial volume is increasing in extent that it is able to issuing the mechanical signals to neighboring structures. Because of the extreme dimensions and asymmetry of neurons, their energetic demands are distributed very heterogeneously over long distances that preclude efficient delivery by diffusion. Mitochondria are therefore actively shuttling along microtubules carried by motor proteins such as kinesin and dynein and tend to concentrate to regions where the demand for mitochondrial function is highest. However, it should be considered that this traffic occurs in narrow neurites with diameter ranging between 150–300 nm that matches with diameter of mitochondria in normal conditions. On the other hand, mitochondria which have opened potassium channels or loosed their membrane potential are having more than twice higher diameter ranging up to 800 nm. It could be thus suggested that increased mitochondrial volume and resulting remodelling of mitochondrial morphology could produce mechanical constraints and decelerate the mitochondrial traffic in neurites. Another possibility is that the geometry remodelling decreases the number of potential contact sites that motor proteins can use to carry the mitochondria along the microtubules. Could this be the one of the mechanisms which coordinates the mitochondrial traffic? We propose that the mitochondrial volume could serve as a fine tuning factor regulating mitochondrial recruitment to regions with high energy needs. High ADP/ATP ratio characteristic to these regions have shown to be responsible for opening of mitochondrial  $K_{ATP}$  channels and decreased mitochondrial membrane potential that both increase the mitochondrial volume. Increased volume leads to remodeling of mitochondrial morphology and decelerates the mitochondrial movement in these regions. As a result the number of mitochondria in the region increases and the energy supply improves. In response to decreased ADP/ATP ratio, the mitochondrial volume decreases and mitochondria are free to leave the region.

## CONCLUSIONS

1. Mitochondria in saponin-treated cerebellar granule cells are structurally intact and functionally preserved in terms of both the respiratory activity and membrane potential. The permeabilized neuronal cultures may be used as a test system for engineering of new pharmacological agents to correct the pathological states of the brain cells.
2. Neurosteroids protect neuronal mitochondria from  $\text{Ca}^{2+}$  overload by inhibiting  $\text{Ca}^{2+}$  influx into the mitochondrial matrix.
3. A decline in mitochondrial membrane potential produces rapid and substantial increase in volume of neuronal mitochondria. Furthermore, these changes could be physiologically relevant as twofold increase in mitochondrial volume and accompanying remodeling of mitochondrial morphology affects the mitochondrial traffic in neurites.



## REFERENCES

- Alexander C, Votruba M, Pesch UE, Thiselton DL, Mayer S, Moore A, Rodriguez M, Kellner U, Leo-Kottler B, Auburger G, Bhattacharya SS, Wissinger B. OPA1, encoding a dynamin-related GTPase, is mutated in autosomal dominant optic atrophy linked to chromosome 3q28. *Nat Genet.* 2000 Oct;26(2):211–5
- Atlante A, Gagliardi S, Marra E, Calissano P, Passarella S. Glutamate neurotoxicity in rat cerebellar granule cells involves cytochrome c release from mitochondria and mitochondrial shuttle impairment. *J Neurochem* 1999;73:237–46.
- Atlante A, Gagliardi S, Marra E, Calissano P. Neuronal apoptosis in rats is accompanied by rapid impairment of cellular respiration and is prevented by scavengers of reactive oxygen species. *Neurosci Lett* 1998;245:127–30.
- Bastianetto S, Ramassamy C, Poirier J, Quirion R. Dehydroepiandrosterone (DHEA) protects hippocampal cells from oxidative stress-induced damage. *Brain Res Mol Brain Res.* 1999 Mar 20;66(1–2):35–41
- Baulieu EE, Thomas G, Legrain S, Lahlou N, Roger M, Debuire B, Faucounau V, Girard L, Hervy MP, Latour F, Leaud MC, Mokrane A, Pitti-Ferrandi H, Triville C, de Lacharriere O, Nouveau S, Rakoto-Arison B, Souberbielle JC, Raison J, Le Bouc Y, Raynaud A, Girerd X, Forette F. Dehydroepiandrosterone (DHEA), DHEA sulfate, and aging: contribution of the DHEAge Study to a sociobiomedical issue. *Proc Natl Acad Sci U S A.* 2000 Apr 11;97(8):4279–84
- Baulieu EE. Neurosteroids: a novel function of the brain. *Psychoneuroendocrinology.* 1998 Nov;23(8):963–87
- Beal MF. Energetics in the pathogenesis of neurodegenerative diseases. *Trends Neurosci.* 2000 Jul;23(7):298–304
- Bixo M, Andersson A, Winblad B, Purdy RH, Backstrom T. Progesterone, 5alpha-pregnane-3,20-dione and 3alpha-hydroxy-5alpha-pregnane-20-one in specific regions of the human female brain in different endocrine states. *Brain Res.* 1997 Aug 1;764(1–2):173–8.
- Cai Q, Gerwin C, Sheng ZH. Syntabulin-mediated anterograde transport of mitochondria along neuronal processes. *J Cell Biol.* 2005 Sep 12;170(6):959–69
- Cardounel A, Regelson W, Kalimi M. Dehydroepiandrosterone protects hippocampal neurons against neurotoxin-induced cell death: mechanism of action. *Proc Soc Exp Biol Med.* 1999 Nov;222(2):145–9
- Cascio C, Prasad VV, Lin YY, Lieberman S, Papadopoulos V. Detection of P450c17-independent pathways for dehydroepiandrosterone (DHEA) biosynthesis in brain glial tumor cells. *Proc Natl Acad Sci U S A.* 1998 Mar 17;95(6):2862–7
- Chen H, Chan DC. Emerging functions of mammalian mitochondrial fusion and fission. *Hum Mol Genet.* 2005 Oct 15;14 Spec No. 2:R283–9
- Compagnone NA, Bulfone A, Rubenstein JL, Mellon SH. Steroidogenic enzyme P450c17 is expressed in the embryonic central nervous system. *Endocrinology.* 1995 Nov;136(11):5212–23
- Corpechot C, Robel P, Axelson M, Sjoval J, Baulieu EE. Characterization and measurement of dehydroepiandrosterone sulfate in rat brain. *Proc Natl Acad Sci U S A.* 1981 Aug;78(8):4704–7

- Crompton M. The mitochondrial permeability transition pore and its role in cell death. *Biochem J.* 1999 Jul 15;341 ( Pt 2):233–49
- Damschroder-Williams PJ, Du J, Chen W, Falke CS, Wei Y, Ito W, Alesci S, Manji HK. Trafficking of estrogen receptor alpha into mitochondria and regulation of mitochondrial function in cultured hippocampal neurons. Program No 403.15. 2005 Abstract Viewer/Itinerary Planner. Washington, DC: Society for Neuroscience
- Das M, Parker JE, Halestrap AP. Matrix volume measurements challenge the existence of diazoxide/glibenclamide-sensitive KATP channels in rat mitochondria. *J Physiol.* 2003 Mar 15;547(Pt 3):893–902
- Davey GP, Canevari L, Clark JB. Threshold effects in synaptosomal and nonsynaptic mitochondria from hippocampal CA1 and paramedian neocortex brain regions. *J Neurochem.* 1997 Dec;69(6):2564–70.
- Davey GP, Peuchen S, Clark JB. Energy thresholds in brain mitochondria. Potential involvement in neurodegeneration. *J Biol Chem.* 1998 May 22;273(21):12753–7
- Dedov VN, Cox GC, Roufogalis BD. Visualization of mitochondria in living neurons with single- and two-photon fluorescence laser microscopy. *Micron* 2001;32:653–60.
- Endo M, Kitazawa T. E-C coupling studies in skinned cardiac fibers. In: Morad M (edit). *Biophysical Aspects of Cardiac Muscle*, Academic, New York, 1978 pp 307–327
- Frey TG, Renken CW, Perkins GA. Insight into mitochondrial structure and function from electron tomography. *Biochim Biophys Acta.* 2002 Sep 10;1555(1–3):196–203
- Furukawa A, Miyatake A, Ohnishi T, Ichikawa Y. Steroidogenic acute regulatory protein (StAR) transcripts constitutively expressed in the adult rat central nervous system: colocalization of StAR, cytochrome P-450SCC (CYP XIA1), and 3beta-hydroxysteroid dehydrogenase in the rat brain. *J Neurochem.* 1998 Dec;71(6):2231–8
- Gallo V, Ciotti MT, Coletti A, Aloisi F, Levi G. Selective release of glutamate from cerebellar granule cells differentiating in culture. *Proc Natl Acad Sci U S A* 1982;79:7919–23.
- Gao W, Pu Y, Luo KQ, Chang DC. Temporal relationship between cytochrome c release and mitochondrial swelling during UV-induced apoptosis in living HeLa cells. *J Cell Sci.* 2001 Aug;114(Pt 15):2855–62
- Garlid KD, Paucek P. Mitochondrial potassium transport: the K(+) cycle. *Biochim Biophys Acta.* 2003 Sep 30;1606(1–3):23–41
- Gleyzer N, Vercauteren K, Scarpulla RC. Control of mitochondrial transcription specificity factors (TFB1M and TFB2M) by nuclear respiratory factors (NRF-1 and NRF-2) and PGC-1 family coactivators. *Mol Cell Biol.* 2005 Feb;25(4):1354–66
- Gogvadze V, Robertson JD, Enoksson M, Zhivotovsky B, Orrenius S. Mitochondrial cytochrome c release may occur by volume-dependent mechanisms not involving permeability transition. *Biochem J.* 2004 Feb 15;378(Pt 1):213–7
- Golden GA, Rubin RT, Mason RP. Steroid hormones partition to distinct sites in a model membrane bilayer: direct demonstration by small-angle X-ray diffraction. *Biochim Biophys Acta.* 1998 Jan 19;1368(2):161–6
- Griparic L, van der Wel NN, Orozco IJ, Peters PJ, van der Bliek AM. Loss of the intermembrane space protein Mgm1/OPA1 induces swelling and localized constrictions along the lengths of mitochondria. *J Biol Chem.* 2004 Apr 30;279(18):18792–8

- Grover GJ, Garlid KD. ATP-Sensitive potassium channels: a review of their cardio-protective pharmacology. *J Mol Cell Cardiol.* 2000 Apr;32(4):677–95
- Guérin B. Mitochondria. In Rose AH, Harrison JS, editors. *The yeasts.* Academic Press: London, 1991;541–600
- Gunter KK, Zuscik MJ, Gunter TE. The Na(+)-independent Ca<sup>2+</sup> efflux mechanism of liver mitochondria is not a passive Ca<sup>2+</sup>/2H<sup>+</sup> exchanger. *J Biol Chem.* 1991 Nov 15;266(32):21640–8
- Gunter TE, Buntinas L, Sparagna G, Eliseev R, Gunter K. Mitochondrial calcium transport: mechanisms and functions. *Cell Calcium.* 2000 Nov-Dec;28(5–6):285–96
- Gähwiler BH, Capogna M, Debanne D, McKinney RA, Thompson SM. Organotypic slice cultures: a technique has come of age. *Trends Neurosci* 1997;20:471–77.
- Halestrap AP. The regulation of the matrix volume of mammalian mitochondria in vivo and in vitro and its role in the control of mitochondrial metabolism. *Biochim Biophys Acta.* 1989 Mar 23;973(3):355–82
- He L, Lemasters JJ. Regulated and unregulated mitochondrial permeability transition pores: a new paradigm of pore structure and function? *FEBS Lett.* 2002 Feb 13; 512(1–3):1–7
- Hollenbeck PJ. The pattern and mechanism of mitochondrial transport in axons. *Front Biosci.* 1996 Jul 1;1:d91–102
- Horvat A, Nikezic G, Petrovic S, Kanazir DT. Binding of estradiol to synaptosomal mitochondria: physiological significance. *Cell Mol Life Sci.* 2001 Apr;58(4):636–44
- Jouaville LS, Pinton P, Bastianutto C, Rutter GA, Rizzuto R. Regulation of mitochondrial ATP synthesis by calcium: evidence for a long-term metabolic priming. *Proc Natl Acad Sci U S A.* 1999 Nov 23;96(24):13807–12
- Kaasik A, Kalda A, Jaako K, Zharkovsky A. Dehydroepiandrosterone sulphate prevents oxygen-glucose deprivation-induced injury in cerebellar granule cell culture. *Neuroscience.* 2001;102(2):427–32
- Kahlert S, Reiser G. Swelling of mitochondria in cultured rat hippocampal astrocytes is induced by high cytosolic Ca(2+) load, but not by mitochondrial depolarization. *FEBS Lett.* 2002 Oct 9;529(2–3):351–5
- Kim HJ, Kang SS, Cho GJ, Choi WS. Steroidogenic acute regulatory protein: its presence and function in brain neurosteroidogenesis. *Arch Histol Cytol.* 2004 Dec; 67(5):383–92
- King SR, Ronen-Fuhrmann T, Timberg R, Clark BJ, Orly J, Stocco DM. Steroid production after in vitro transcription, translation, and mitochondrial processing of protein products of complementary deoxyribonucleic acid for steroidogenic acute regulatory protein. *Endocrinology.* 1995 Nov;136(11):5165–76
- Kohchi C, Ukena K, Tsutsui K. Age- and region-specific expressions of the messenger RNAs encoding for steroidogenic enzymes p450scc, P450c17 and 3β-HSD in the postnatal rat brain. *Brain Res.* 1998 Aug 10;801(1–2):233–8.
- Kokoszka JE, Waymire KG, Levy SE, Sligh JE, Cai J, Jones DP, MacGregor GR, Wallace DC. The ADP/ATP translocator is not essential for the mitochondrial permeability transition pore. *Nature.* 2004 Jan 29;427(6973):461–5
- Kroemer G, Reed JC. Mechanisms of mitochondrial membrane permeabilization. *Cell Death Differ.* 2000 Dec;7(12):1145
- Kudin A, Vielhaber S, Beck H, Elger CE, Kunz WS. Quantitative investigation of mitochondrial function in single rat hippocampal slices: a novel application of high-

- resolution respirometry and laser-excited fluorescence spectroscopy. *Brain Res Protocols* 1999;4:329–34.
- Kunz WS. Different metabolic properties of mitochondrial oxidative phosphorylation in different cell types – important implications for mitochondrial cytopathies. *Exp Physiol*. 2003 Jan;88(1):149–54
- Lacroix C, Fiet J, Benais JP, Gueux B, Bonete R, Villette JM, Gourmel B, Dreux C. Simultaneous radioimmunoassay of progesterone, androst-4-enedione, pregnenolone, dehydroepiandrosterone and 17-hydroxyprogesterone in specific regions of human brain. *J Steroid Biochem*. 1987 Sep;28(3):317–25
- Lasorsa FM, Pinton P, Palmieri L, Fiermonte G, Rizzuto R, Palmieri F. Recombinant expression of the Ca(2+)-sensitive aspartate/glutamate carrier increases mitochondrial ATP production in agonist-stimulated Chinese hamster ovary cells. *J Biol Chem*. 2003 Oct 3;278(40):38686–92
- Lee CP. Biochemical studies of isolated mitochondria from normal and diseased tissues. *Biochim Biophys Acta*. 1995 May 24;1271(1):21–8
- Lee KD, Hollenbeck PJ. Phosphorylation of kinesin in vivo correlates with organelle association and neurite outgrowth. *J Biol Chem*. 1995 Mar 10;270(10):5600–5
- Leist M, Nicotera P. Calcium and neuronal death. *Rev Physiol Biochem Pharmacol*. 1998;132:79–125
- Li H, Papadopoulos V. Peripheral-type benzodiazepine receptor function in cholesterol transport. Identification of a putative cholesterol recognition/interaction amino acid sequence and consensus pattern. *Endocrinology*. 1998 Dec;139(12):4991–7. 1998
- Li Z, Okamoto K, Hayashi Y, Sheng M. The importance of dendritic mitochondria in the morphogenesis and plasticity of spines and synapses. *Cell*. 2004 Dec 17;119(6):873–87
- Ligon LA, Steward O. Role of microtubules and actin filaments in the movement of mitochondria in the axons and dendrites of cultured hippocampal neurons. *J Comp Neurol*. 2000 Nov 20;427(3):351–61
- Liu J, Li H, Papadopoulos V. PAP7, a PBR/PKA-R1alpha-associated protein: a new element in the relay of the hormonal induction of steroidogenesis. *J Steroid Biochem Mol Biol*. 2003 Jun;85(2–5):275–83.
- Lyamzaev KG, Izumov DS, Avetisyan AV, Yang F, Pletjushkina OY, Chernyak BV. Inhibition of mitochondrial bioenergetics: the effects on structure of mitochondria in the cell and on apoptosis. *Acta Biochim Pol*. 2004;51(2):553–62
- Maayan R, Touati-Werner D, Ram E, Galdor M, Weizman A. Is brain dehydroepiandrosterone synthesis modulated by free radicals in mice? *Neurosci Lett*. 2005 Mar 29;377(2):130–5
- Mandelkow EM, Thies E, Trinczek B, Biernat J, Mandelkow E. MARK/PAR1 kinase is a regulator of microtubule-dependent transport in axons. *J Cell Biol*. 2004 Oct 11;167(1):99–110
- Masri RK. Estradiol- and progesterone-mediated mitochondrial regulation. Program No 633.14. 2005 Abstract Viewer/Itinerary Planner. Washington, DC: Society for Neuroscience.
- Mattson MP, Robinson N, Guo Q. Estrogens stabilize mitochondrial function and protect neural cells against the pro-apoptotic action of mutant presenilin-1. *Neuroreport*. 1997 Dec 1;8(17):3817–21
- McCormack JG, Halestrap AP, Denton RM. Role of calcium ions in regulation of mammalian intramitochondrial metabolism. *Physiol Rev*. 1990 Apr;70(2):391–425

- Miller WL. Minireview: regulation of steroidogenesis by electron transfer. *Endocrinology*. 2005 Jun;146(6):2544–50
- Minamikawa T, Williams DA, Bowser DN, Nagley P. Mitochondrial permeability transition and swelling can occur reversibly without inducing cell death in intact human cells. *Exp Cell Res*. 1999 Jan 10;246(1):26–37
- Mohan PF, Cleary MP. Dehydroepiandrosterone and related steroids inhibit mitochondrial respiration in vitro. *Int J Biochem*. 1989;21(10):1103–7
- Mootha VK, Bunkenborg J, Olsen JV, Hjerrild M, Wisniewski JR, Stahl E, Bolouri MS, Ray HN, Sihag S, Kamal M, Patterson N, Lander ES, Mann M. Integrated analysis of protein composition, tissue diversity, and gene regulation in mouse mitochondria. *Cell*. 2003 Nov 26;115(5):629–40
- Morin C, Zini R, Simon N, Tillement JP. Dehydroepiandrosterone and alpha-estradiol limit the functional alterations of rat brain mitochondria submitted to different experimental stresses. *Neuroscience*. 2002;115(2):415–24
- Morris RL, Hollenbeck PJ. The regulation of bidirectional mitochondrial transport is coordinated with axonal outgrowth. *J Cell Sci*. 1993 Mar;104 ( Pt 3):917–27
- Moutsatsou P, Psarra AM, Tsiapara A, Paraskevskou H, Davaris P, Sekeris CE. Localization of the glucocorticoid receptor in rat brain mitochondria. *Arch Biochem Biophys*. 2001 Feb 1;386(1):69–78.
- Muneyuki E, Makino M, Kamata H, Kagawa Y, Yoshida M, Hirata H. Inhibitory effect of Na<sub>3</sub>N on the F<sub>0</sub>F<sub>1</sub> ATPase of submitochondrial particles as related to nucleotide binding. *Biochim Biophys Acta*. 1993 Aug 16;1144(1):62–8
- Nicholls DG, Budd SL. Mitochondria and neuronal survival. *Physiol Rev*. 2000 Jan; 80(1):315–60
- O'Rourke. Pathophysiological and protective roles of mitochondrial ion channels. *J Physiol*. 2000 Nov 15;529 Pt 1:23–36
- Ozawa T, Sako Y, Sato M, Kitamura T, Umezawa Y. A genetic approach to identifying mitochondrial proteins. *Nat Biotechnol*. 2003 Mar;21(3):287–93
- Overly CC, Rieff HI, Hollenbeck PJ. Organelle motility and metabolism in axons vs dendrites of cultured hippocampal neurons. *J Cell Sci*. 1996 May;109 ( Pt 5):971–80
- Papadopoulos V, Amri H, Boujrad N, Cascio C, Culty M, Garnier M, Hardwick M, Li H, Vidic B, Brown AS, Reversa JL, Bernassau JM, Drieu K. Peripheral benzodiazepine receptor in cholesterol transport and steroidogenesis. *Steroids*. 1997 Jan; 62(1):21–8
- Rintoul GL, Filiano AJ, Brocard JB, Kress GJ, Reynolds IJ. Glutamate decreases mitochondrial size and movement in primary forebrain neurons. *J Neurosci*. 2003 Aug 27;23(21):7881–8
- Rosignol R, Letellier T, Malgat M, Rocher C, Mazat JP. Tissue variation in the control of oxidative phosphorylation: implication for mitochondrial diseases. *Biochem J*. 2000 Apr 1;347 Pt 1:45–53
- Saks VA, Veksler VI, Kuznetsov AV, Kay L, Sikk P, Tiivel T, Tranqui L, Olivares J, Winkler K, Wiedemann F, Kunz WS. Permeabilized cell and skinned fiber techniques in studies of mitochondrial function in vivo. *Mol Cell Biochem* 1998;184:81–100.
- Sanne JL, Krueger KE. Expression of cytochrome P450 side-chain cleavage enzyme and 3 beta-hydroxysteroid dehydrogenase in the rat central nervous system: a study by polymerase chain reaction and in situ hybridization. *J Neurochem*. 1995 Aug; 65(2):528–36.

- Sato-Harada R, Okabe S, Umeyama T, Kanai Y, Hirokawa N. Microtubule-associated proteins regulate microtubule function as the track for intracellular membrane organelle transports. *Cell Struct Funct.* 1996 Oct;21(5):283–95
- Schon EA, Manfredi G. Neuronal degeneration and mitochondrial dysfunction. *J Clin Invest.* 2003 Feb;111(3):303–12
- Shepherd GM, Harris KM. Three-dimensional structure and composition of CA3–>CA1 axons in rat hippocampal slices: implications for presynaptic connectivity and compartmentalization
- Shibuya K, Takata N, Hojo Y, Furukawa A, Yasumatsu N, Kimoto T, Enami T, Suzuki K, Tanabe N, Ishii H, Mukai H, Takahashi T, Hattori TA, Kawato S. Hippocampal cytochrome P450s synthesize brain neurosteroids which are paracrine neuromodulators of synaptic signal transduction. *Biochim Biophys Acta.* 2003 Feb 17;1619(3):301–16
- Sierra A. Neurosteroids: the StAR protein in the brain. *J Neuroendocrinol.* 2004 Sep;16(9):787–93
- Sims NR, Anderson MF. Mitochondrial contributions to tissue damage in stroke. *Neurochem Int.* 2002 May;40(6):511–26
- Smirnova E, Griparic L, Shurland DL, van der Bliek AM. Dynamin-related protein Drp1 is required for mitochondrial division in mammalian cells. *Mol Biol Cell.* 2001 Aug;12(8):2245–56
- Stock D, Leslie AG, Walker JE. Molecular architecture of the rotary motor in ATP synthase. *Science.* 1999 Nov 26;286(5445):1700–5
- Stojanovski D, Koutsopoulos OS, Okamoto K, Ryan MT. Levels of human Fis1 at the mitochondrial outer membrane regulate mitochondrial morphology. *J Cell Sci.* 2004 Mar 1;117(Pt 7):1201–10
- Stromstedt M, Waterman MR. Messenger RNAs encoding steroidogenic enzymes are expressed in rodent brain. *Brain Res Mol Brain Res.* 1995 Dec 1;34(1):75–88
- Taylor RW, Turnbull DM. Mitochondrial DNA mutations in human disease. *Nat Rev Genet.* 2005 May;6(5):389–402
- Tatton WG, Olanow CW. Apoptosis in neurodegenerative diseases: the role of mitochondria. *Biochim Biophys Acta.* 1999 Feb 9;1410(2):195–213
- Thorburn DR. Diverse powerhouses. *Nat Genet.* 2004 Jan;36(1):13–4
- Tsutsui K, Sakamoto H, Ukena K. Biosynthesis and action of neurosteroids in the cerebellar Purkinje neuron. *J Steroid Biochem Mol Biol.* 2003 Jun;85(2–5):311–21
- Vasilyeva EA, Minkov IB, Fitin AF, Vinogradov AD. Kinetic mechanism of mitochondrial adenosine triphosphatase. Inhibition by azide and activation by sulphite. *Biochem J.* 1982 Jan 15;202(1):15–23
- Veksler VI, Kuznetsov AV, Sharov VG, Kapelko VI, Saks VA. Mitochondrial respiratory parameters in cardiac tissue: a novel method of assessment by using saponin-skinned fibers. *Biochim Biophys Acta* 1987;892:191–6.
- Wang J, Green PS, Simpkins JW. Estradiol protects against ATP depletion, mitochondrial membrane potential decline and the generation of reactive oxygen species induced by 3-nitropropionic acid in SK-N-SH human neuroblastoma cells. *J Neurochem.* 2001 May;77(3):804–11
- Weill-Engerer S, David JP, Sazdovitch V, Liere P, Eychenne B, Pianos A, Schumacher M, Delacourte A, Baulieu EE, Akwa Y. Neurosteroid quantification in human brain regions: comparison between Alzheimer's and nondemented patients. *J Clin Endocrinol Metab.* 2002 Nov;87(11):5138–43

- Westermann B. Merging mitochondria matters: cellular role and molecular machinery of mitochondrial fusion. *EMBO Rep.* 2002 Jun;3(6):527–31
- Wustmann C, Petzold D, Fischer HD, Kunz W. ATP-metabolizing enzymes in suspensions of isolated coupled rat brain mitochondria. *Biomed Biochim Acta.* 1987;46(5):331–40
- Yang SY, He XY, Schulz H. Fatty acid oxidation in rat brain is limited by the low activity of 3-ketoacyl- coenzyme A thiolase. *J Biol Chem.* 1987 262, 13027–32
- Yoon Y, McNiven MA. Mitochondrial division: New partners in membrane pinching. *Curr Biol.* 2001 Jan 23;11(2):R67–70
- Zheng J, Ramirez VD. Purification and identification of an estrogen binding protein from rat brain: oligomycin sensitivity-conferring protein (OSCP), a subunit of mitochondrial F0F1-ATP synthase/ATPase. *J Steroid Biochem Mol Biol.* 1999 Jan;68(1–2):65–75
- Zuchner S, Mersyanova IV, Muglia M, Bissar-Tadmouri N, Rochelle J, Dadali EL, Zappia M, Nelis E, Patitucci A, Senderek J, Parman Y, Evgrafov O, Jonghe PD, Takahashi Y, Tsuji S, Pericak-Vance MA, Quattrone A, Battaloglu E, Polyakov AV, Timmerman V, Schroder JM, Vance JM. Mutations in the mitochondrial GTPase mitofusin 2 cause Charcot-Marie-Tooth neuropathy type 2A. *Nat Genet.* 2004 May;36(5):449–51.

## SUMMARY IN ESTONIAN

### **Mitokondrid väikeaju granulaarrakkude kultuuris: mitokondrite funktsiooni iseloomustus, mahu regulatsiooni mehhanismid ning interaktsioonid neurosteroididega**

Mitokondrites toimuv oksüdatiivne fosforüülimine on närvirakkude peamine energiaallikas. Neuronid on, polaarsed rakud ning mitokondrid paiknevad nii rakukehas kui jätketes. Mitokondrite normaalne funktsioneerimine ning liikumine jätketes on vajalik energia varustuse tagamiseks kõigis neuronis osades. Lisaks energiaproduktioonile osalevad mitokondrid ka programmeeritud rakusurma protsessis vabastades kahjustuse korral apoptoosi käivitavaid valke. Mitokondrid osalevad ka rakusisese kaltsiumi homöostaasi regulatsioonis. Mitokondrite tähtsus raku homöostaasis selgitab ka seda, miks mitokondrite funktsiooni häireid seostatakse mitmete patoloogiatega. Mitmed neurodegeneratiivsed haigused on seostatavad häiretega oksüdatiivses fosforüülimises (Parkinsoni tõbi), mitokondriaalse DNA mutatsioonidega (Leberi nägemisnärv atroofia) või häiretega mitokondrite aksonaalses transpordis (Huntingtoni tõbi, Alzheimeri tõbi).

Mitokondrites toimub osaliselt ka steroidhormoonide süntees. Kuigi steroidide sünteesis osalevate tsütokroom p450 ensüümide kõrge aktiivsus on omane peamiselt steroidogeensetele kudedele, sünteesitakse mitmeid steroide ka ajus, nii gliia kui ka neuronite poolt. Neid, nn. neurosteroide peetakse neuroprotektiivseteks ning nende toime ei avaldu mitte ainult genoomsete mehhanismide kaudu, vaid tulenevalt interaktsioonidest raku pinna retseptoritega või ka mitokondritega.

Võrreldes teiste kudede mitokondritega on neuronaalsetel mitokondritel mitmeid eripärasid. Kuigi enamik teadmisi neuronaalsete mitokondrite funktsioonist põhinevad katsetel isoleeritud mitokondritega, ei võimalda need tehnikad uurida spetsiifiliselt neuronite mitokondreid, sest ligi pool aju rakkudest on gliia rakud. Samuti saab mitondrite isoleerimise käigus kahjustada mitokondrite struktuuri.

### *Töö eesmärgid ja tulemused*

1. Rakendada selektiivse permeabiliseerimise meetodit mitokondrite funktsiooni uurimiseks primaarsetes neuronaalsetes kultuurides *in situ*:  
Rakukultuuris kasvatatud väikeaju granulaarrakke töödeldi saponiiniga, mis permeabiliseeris rakkude plasmamembraani, kuid jättis mitokondrite membraanid intaktseks. Mitokondrite funktsionaalsust permeabiliseeritud neuronites hinnati mõõtes mitokondrite membraanipotentsiaali, kaltsiumi akumulendumis-



võimet ning hapnikutarbimist. Tulemused näitasid, et mitokondrid säilitavad permeabiliseeritud plasmamembraaniga neuronites intaktsuse: säilib nii hapikutarbimine, membraanipotentsiaal ning kaltsiumi akumulereerimisvõime.

2. Selgitada kas neurosteroidid mõjutavad neuronaalsete mitokondrite funktsiooni.

Neurosteroidide võimalikku protektiivset toimet uuriti premeabiliseeritud neuronites kaltsiumi ülekoormuse mudelis. Tulemused näitasid, et nii dehidroepiandrosteroon kui ka mitmed teised neurosteroidid kaitsevad neuronaalseid mitokondreid tsütoplasmaatilise kaltsiumi ülekoormuse eest takistades mitokondri membraanipotentsiaali langust ja kaltsiumi üleliigset akumulereerumist mitokondri maatriksisse.

3. Selgitada mitokondrite mahu regulatsiooni mehhanisme ja selle võimalikku füsioloogilist tähendust neuronites:

Mitokondrid märgistati permeabiliseeritud neuronites fluorestsentsmarker MitoTracker Green'ga ning nende morfoloogiline analüüs teostati laserkonfokaalmikroskoopia ja dekonvolutsiooni meetodi abil. Tulemused näitasid, et mitokondrite maht muutub mitokondrite membraanipotentsiaali ja kaaliumi-voolude muutumisel. Samuti viitavad tulemused sellele, et mitokondri mahu suurenemisel aeglustub mitokondrite transport neuronaalsetes jätketes.

### *Järeldused*

1. Mitokondrid säilitavad permeabiliseeritud väikeaju granulaarrakkude kultuuris struktuurse terviklikkuse ja funktsiooni – säilib respiratoorne aktiivsus ning membraanipotentsiaal. Permeabiliseeritud neuronaalne kultuur on seega sobivaks mudeliks farmakonide toimemehhanismide uurimiseks.
2. Neurosteroidid kaitsevad mitokondreid kaltsiumi ülekoormuse eest inhibeerides kaltsiumi sissevoolu mitokondrisse.
3. Mitokondrite membraanipotentsiaali langus põhjustab kiire ja olulise mitokondrite mahu suurenemise, mis pärssib nende organellide liikumise neuronaalsetes jätketes.

## ACKNOWLEDGEMENTS

This study was carried out at the Department of Pharmacology, University of Tartu in collaboration with the Department of Patophysiology, during the years 2001–2005. The study was funded by grants from Estonian Science Foundation.

I would like to thank all my colleagues from Department of Pharmacology for their help and support:

My supervisors, Prof. Alexander Zharkovsky and Dr. Allen Kaasik for their teaching and encouragement;

Ulla Peterson and Oili Suvi for their excellent technical assistance;

Dr. Paavo Pokk and Dr. Anti Kalda for inspirative discussions about life and science;

I am grateful to my collaborators from Department of Patophysiology, Prof. Enn Seppet and Nadezhda Peet;

I highly appreciate the contribution of Prof. Vladimir Veksler to this work;

My deepest thanks go to my family who always supported me.

Finally, I would like to thank the Center of Molecular and Clinical Medicine for travel scholarships.

## **PUBLICATIONS**

Kaasik A, Safiulina D, Kalda A, Zharkovsky A.  
Dehydroepiandrosterone with other neurosteroids preserve  
neuronal mitochondria from calcium overload.  
*The Journal of Steroid Biochemistry and Molecular Biology*,  
2003 Okt; 87(1): 97–103

Safiulina D, Kaasik A, Seppet E, Peet N, Zharkovsky A, Seppet E.  
Method for in situ detection of the mitochondrial function in neurons.  
*Journal of Neuroscience Methods*, 2004 Aug; 137(1):87–95

Safiulina D, Veksler V, Zharkovsky A, Kaasik A.  
Loss of mitochondrial membrane potential is associated with increase  
in mitochondrial volume: physiological role in neurons.  
*Journal of Cellular Physiology*. 2006 Feb; 206(2): 347–53

# CURRICULUM VITAE

## **Dzhamilja Safiulina**

|                         |                           |
|-------------------------|---------------------------|
| Citizenship             | Estonian                  |
| Date and place of birth | November 28, 1978, Russia |
| Address                 | Koidula 14–4, Tartu 51006 |
| Phone                   | +372 737 4359             |
| E-mail                  | dzamilja.safiulina@ut.ee  |

### Education

|           |  |
|-----------|--|
| 1985–1996 | Tartu Slavian Secondary School   |
| 1996–2001 | University of Tartu, Faculty of Medicine, BSc in Pharmacy                  |
| 2001–2006 | University of Tartu, Faculty of Medicine, Doctoral Program in Neuroscience |

### Professional employment

|           |  |
|-----------|--|
| 2000–2001 | University of Tartu, Department of Pharmacology, laboratory technician   |
| 2004–     | University of Tartu, Department of Pharmacology teaching assistant (0.5) |

### Scientific work

Brain bioenergetics: role of mitochondria in neuronal function and dysfunction.

# ***CURRICULUM VITAE***

## **Džamilja Safiulina**

|                  |                            |
|------------------|----------------------------|
| Kodakondsus      | Eesti                      |
| Sünniaeg ja koht | 28. november 1978, Venemaa |
| Aadress          | Koidula 14–4, Tartu 51006  |
| Telefon          | +372 737 4359              |
| E-mail           | dzamilja.safiulina@ut.ee   |

### Haridus

|           |  |
|-----------|--|
| 1985–1996 | Tartu Slaavi Gümnaasium                                  |
| 1996–2001 | Tartu Ülikool, Arstiteaduskond, Proviisoriõpe (BSc)      |
| 2001–2006 | Tartu Ülikool, Arstiteaduskond, Neuroteaduste doktoriõpe |

### Teenistuskäik

|           |   |
|-----------|---|
| 2000–2001 | Tartu Ülikool, Farmakoloogia Instituut, laborant        |
| 2004–     | Tartu Ülikool, Farmakoloogia Instituut, assistent (0.5) |

### Teadustöö

Aju bioenergeetika: mitokondrite roll neuronite funktsioonis ja düsfunktsioonis.